Nuclear translocation of p85β promotes tumorigenesis of PIK3CA helical domain mutant cancer

Yujun Hao
Shanghai Jiao Tong University School of medicine
Baoyu He
Shanghai Jiao Tong University School of medicine
Liping Wu
Case Western Reserve University
Yamu Li
Case Western Reserve University
Chao Wang
National Cancer Centre
Ting Wang
Shanghai Jiao Tong University School of medicine
Longci Sun
Shanghai Jiao Tong University School of medicine
Yanhua Zhang
Shanghai Jiao Tong University School of medicine
Yangyang Zhan
Second Military Medical University https://orcid.org/0000-0003-3394-5070
Yiqing Zhao
Case Western Reserve University
Sanford Markowitz
Case Western Reserve University
Martina Veigl
Case Western Reserve University
Ronald Conlon
Case Western Reserve University
Zhenghe Wang (zxw22@case.edu)
Case Western Reserve University

Article

Keywords: PIK3CA, p85β, tumorigenesis

Posted Date: May 5th, 2021

DOI: https://doi.org/10.21203/rs.3.rs-462020/v1

Version of Record: A version of this preprint was published at Nature Communications on April 13th, 2022. See the published version at https://doi.org/10.1038/s41467-022-29585-x.

Nuclear translocation of p85β promotes tumorigenesis of PIK3CA helical domain mutant cancer

Yujun Hao[1,2,3 *, #], Baoyu He[1, *], Liping Wu[2,3,4, *], Yamu Li[2,3,*], Chao Wang[2, 3], Ting Wang[1], Longci Sun[1], Yanhua Zhang[1], Yangyang Zhan[1], Yiqing Zhao[2,3], Sanford Markowitz[3,5], Martina Veigl[3], Ronald A. Conlon[2,3], Zhenghe Wang[2,3, #]

[1] State Key Laboratory of Oncogenes and Related Genes, Shanghai Cancer Institute, Renji Hospital, Shanghai Jiao Tong University School of Medicine, 200032 Shanghai, China

[2] Department of Genetics and Genome Sciences,

[3] Case Comprehensive Cancer Center,

[5]Department of Medicine,

School of Medicine, Case Western Reserve University, 10900 Euclid Avenue, Cleveland, Ohio 44106 USA

[4] Department of Chemistry, College of Basic Medical Sciences,

Army Medical University (Third Military Medical University) Chongqing, 400038, P. R. China.

[*] These authors contributed equally.

[#] To whom correspondence should be addressed. Email: yjhao@shsci.org (YH); and zxw22@case.edu (ZW).

Abstract

PI3Ks consist of p110 catalytic subunits and p85 regulatory subunits. PIK3CA, encoding p110α, is frequently mutated in human cancers. Most PIK3CA mutations are clustered in the helical domain or the kinase domain. Here, we report that p85β disassociates from p110α helical domain mutant protein and translocates into the nucleus through a nuclear localization sequence (NLS). Nuclear p85β recruits deubiquitinase USP7 to stabilize EZH1 and EZH2 and enhances H3K27 trimethylation. Knockout of p85β or p85β NLS mutant reduces the growth of tumors harboring a PIK3CA helical domain mutation. Our studies illuminate a novel mechanism by which PIK3CA helical domain mutations exert their oncogenic function. Finally, a combination of Alpelisib, a p110α-specific inhibitor, and an EZH inhibitor, Tazemetostat, induces regression of xenograft tumors harboring a PIK3CA helical domain mutation, but not tumors with either a WT PIK3CA or a PIK3CA kinase domain mutation, suggesting that the drug combination could be an effective therapeutic approach for PIK3CA helical domain mutant tumors.

Introduction

PIK3CA, which encodes the p110α catalytic subunit of PI3 kinase, is one of the most frequently mutated oncogenes in human cancers [1-3]. Recently, the FDA approved the combination of p110α-specific inhibitor Alpelisib and the estrogen receptor antagonist Fulvestrant to treat PIK3CA-mutant breast cancer patients whose tumors are hormone receptor (HR)-positive and HER2-negative [4]. This approval highlights mutant PIK3CA (encoding p110α protein) as a critical cancer drug target and the importance of further understanding the molecular mechanisms by which PIK3CA mutations drive tumorigenesis. PI3Ks are heterodimers consisting of a p110 catalytic subunit and a p85 regulatory subunit [5]. Normally, the p85 subunits bind and stabilize the p110 subunit and inhibit its enzymatic activity [6]. Upon growth factor stimulation, the SH2 domains of p85 bind to the phospho-tyrosine residues on receptor protein kinases or adaptor proteins such as insulin receptor substrate 1 (IRS1), which activates PI3K and catalyzes the conversion of phosphatidylinositol-4,5-bisphosphate (PIP2) to phosphatidylinositol-3,4,5-triphosphate (PIP3) [5]. PIP3 recruits pleckstrin homology domain-containing proteins, including PDK1 and AKTs, to the cell membrane to activate signaling pathways [5].

Most tumor-derived PIK3CA mutations are clustered in two hotspots in p110α protein: the E542, E545, and Q546 residues in the helical domain and the H1047 residue in the kinase domain [1,7]. Accumulating evidence suggests that the helical domain mutations and kinase domain mutations exert their oncogenic functions through distinct molecular mechanisms. p110α helical domain mutations alleviate the inhibitory interaction between p110α and the N-terminal SH2 domain (nSH2) of p85α and β, and facilitate

direct interaction of p110α with IRS1 [8-12]. The E545K helical domain mutation in p110α does not increase lipid kinase activity in response to phosphorylation of receptor tyrosine kinase or adaptor proteins [8,10-12]. Moreover, the p110α E545K helical domain mutant requires the Ras-binding domain to transform chicken embryonic fibroblasts [13], whereas the H1047R kinase domain mutant requires the p85-binding domain. Phenotypically, breast cancer cells expressing a PIK3CA helical domain mutation showed more severe metastatic phenotypes than that of wild-type or PIK3CA H1047R mutation in an isogenic background [14]. Furthermore, patients with a PIK3CA H1047R mutation have a better response to PI3K/AKT/mTOR inhibitors than patients with a PIK3CA helical domain mutation in early phase clinical trials [15,16].

The regulatory subunits of PI3K p85α (encoded by PIK3R1) and p85β (encoded by PIK3R2) are ubiquitously expressed, but they seem to play opposite roles in tumorigenesis [17]. Loss-of-function mutations of p85α frequently occur in endometrial and brain cancers [18,19], suggesting that it normally functions as a tumor suppressor [20,21]. In contrast, p85β often is overexpressed in diverse cancers and depletion of p85β impairs tumor formation in vivo and in vitro [22-26], suggesting that it plays an oncogenic role in tumorigenesis. Intriguingly, several studies have demonstrated that p85 proteins can regulate biological processes through nuclear translocation [27-31]. It has been shown that p85α and p85β interact with nuclear Bromodomain-containing protein 7 (BRD7) and X-box binding protein 1 (XBP1) to regulate glucose homeostasis [30,31]. However, it remains unknown whether nuclear p85 proteins play an important role in tumorigenesis.

We report here that p85β, but not p85α, disassociates from p110α and translocates into the nucleus in cancer cells with a p110α helical domain mutation, thereby promoting

tumor growth. The nuclear p85β recruits deubiquitinase USP7 to stabilize histone methyltransferases EZH1 and EZH2 and enhances histone H3 lysine 27 trimethylation (H3K27Me3). Moreover, we demonstrate that a combination of Alpelisib and an EZH inhibitor, Tazemetostat, induces regression of xenograft tumors harboring a PIK3CA helical domain mutation, but not tumors with either a WT PIK3CA or a PIK3CA kinase domain mutation.

Results

p85β disassociates from p110α helical domain mutant protein.

We previously demonstrated that p110α helical domain mutant proteins (e.g. E545K) gain direct interaction with IRS1 independent of p85α and β, thereby rewiring oncogenic signaling [12]. To gain insights into how the p110α helical domain mutations impact PI3K complex formation, we immunoprecipitated either wild-type (WT) p110α or p110α E545K mutant protein in cell lines with the WT or mutant endogenous p110α proteins tagged with 3×FLAG [[12], Figure 1a]. Interestingly, compared to the WT p110α protein, the p110α E545K protein drastically reduced its binding to p85β, but not p85α (Figures 1b and S1a). This observation was further validated by reciprocal immunoprecipitation of either p85β or p85α in isogenic DLD1 cell lines with either WT-only (PIK3CA E545K allele knockout) or E545K-only (PIK3CA WT allele knockout, Figures 1c, 1d, S1b, and S1c). We postulated that some of the p85β proteins might disassociate from the PI3K complexes in PIK3CA E545K mutant cells. Indeed, immunoprecipitation with both p110α and p110β in the isogenic DLD1 E545K-only and WT-only cells showed more PI3K complex-free (post-IP) p85β were present in the

E545K-only cells than in the WT-only cells (Figure S1c). These results were further validated by gel-filtration analyses (Figure S1e).

Tumor-derived PIK3CA mutations are clustered in two hotspots: one in the helical domain at E542, E545, Q546, and the other in the kinase domain at the H1047 site. We set out to determine which mutations in p110α affect binding to p85β. As shown in Figure 1e, 1f and S1f, as with the p110α E545K mutant, the p110α E542K and Q546K mutant proteins disrupted their interactions with p85β compared to the WT p110α. In contrast, the kinase domain p110α H1047R mutant protein had no impact on p85β binding. Neither did other relative rare p110α mutant proteins including R88Q and K111N in the ABD domain, N345K and C420R in the C2 domain, M1043I and G1049R in the kinase domain (Figures 1e, 1f, and S1f).

We then used six different cell lines to assess p85β-p110 complex formation. Consistently, the interaction between p85β and p110α were weaker in two cell lines with PIK3CA E545K mutation (DLD1 and H460) than in either two cell lines with wild-type PIK3CA (SW480 and LoVo) or two cell lines with PIK3CA H1047R mutation (HCT116 and T47D) (Figures 1g, 1h, S1g, and S1h). In contrast, the interactions between p85β and p110β or between p85α and p110α were similar in these six cell lines (Figures 1g, 1h, S1g, and S1h). Together, our data suggest that the p85β protein dissociates from the mutant p110α in cancer cells with a PIK3CA helical domain mutation.

The N-terminal p85β sequences cause its dissociation from p110α helical domain mutant protein.

It is interesting that p85β, but not p85α, disassociates from the p110α helical domain mutant proteins. A protein sequence alignment showed that the SH3 domain, GAP domain, and link region between the GAP and nSH2 domains in the N-terminus sequences between p85α and p85β are less conserved (56% identical, Figure 1i). In contrast, the three SH2 domains in the two proteins' C-terminus are highly conserved (91% identical, Figure 1i). We postulated that the N-terminus sequences of p85β might cause its disassociation from the p110α helical domain mutant proteins. To this end, we constructed two chimeric p85 proteins that swapped the N-terminus regions of p85α and p85β (Figure 1i). As shown in Figure 1J, the N-terminal p85α-C-terminal p85β chimeric proteins bound similarly to both p110α WT and E545K mutant proteins, whereas the N-terminal p85β-C-terminal p85α chimeric protein bound to less p110α E545K mutant protein compared to the WT counterpart (Figure 1j). These data suggest that the N-terminal sequences of p85β cause its disassociation from the p110α helical domain mutant proteins.

p85β plays an oncogenic role in cancer cells with a PIK3CA helical domain mutation.

To explore the specific function of p85β in p110α helical domain mutated tumors, we assessed whether p85β expression levels are associated with any clinical outcomes. We chose to analyze the following four TCGA datasets because PIK3CA is frequently mutated, and PIK3R2 is overexpressed in these tumor types: colorectal cancer (COAD), bladder carcinoma (BLCA), endometrial carcinoma (UCEC), and breast cancer (BRCA) (Figure S2a). Because the number of patients whose tumors harbor PIK3CA mutations is small in each tumor type, we combined the TCGA data of the four tumor types together and divided the patients into three groups according to the PIK3CA mutation

status: helical domain mutation group, non-helical domain mutation group, and wild-type group. Interestingly, high expression of PIK3R2 was found to be significantly associated with poor five-year survival only in the helical domain mutation group (HR=2.146, 95% CI 1.162~3.96, p=0.0148), but not in the non-helical domain mutation group (HR=0.9126, 95% CI 0.5714~1.4, p=0.7017) or wild-type group (HR=0.9325, 95% CI 0.7404~1.1, p=0.5527) (Figure 2a). These data suggest that p85β may promote tumorigenesis in tumors with a PIK3CA helical domain mutation.

The depletion of p85β reduces the growth of cancer cells with a PIK3CA helical domain mutation, but not cells with WT or a kinase domain mutant PIK3CA.

To further investigate the function of p85β in the context of PIK3CA helical domain mutation, we knocked out p85β in the isogenic DLD1 PIK3CA E545K-only and PIK3CA WT-only cell lines (Figure 2b). As shown in Figures 2c to 2f, knockout of p85β reduced cell proliferation, colony formation, and xenograft tumor growth of the DLD1 PIK3CA E545K-only cells, but not the WT PIK3CA-only counterpart. Similarly, knockdown of p85β reduced cell proliferation and colony formation of PIK3CA E545K mutant MDA-MB361 breast cancer cells and H460 lung cancer cells and PIK3CA E542K mutant SW948 cells (Figures 2g-2i, S2b-S2d). In contrast, knockdown of p85β had no impact on cell proliferation and colony formation of PIK3CA H1047R mutant T47D breast cancer cells and RKO colon cancer cells, or PIK3CA WT SW480 cells (Figures 2g-2i, S2e-S2h). Together, these data suggest that p85β promotes the growth of tumors harboring PIK3CA helical domain mutations, but not those tumors with WT or PIK3CA kinase domain mutations.

p85β translocates into the nucleus in cancer cells with a PIK3CA helical domain

mutation.

Next, we set out to elucidate the molecular mechanisms by which p85β promotes the growth of cancer cells with a PIK3CA helical domain mutation. Given that it is well documented that PI3K transduces signaling to AKT, we examined whether p85β knockout impacts AKT and its downstream signaling. As shown in Figure S3a, knockout of p85β did not affect phosphorylation of AKT, GSK3β, Foxo, mTOR, and p70S6K in DLD1 PIK3CA E545K-only cells regardless of whether under serum starvation conditions or when stimulated by insulin or EGF. Moreover, neither knockout of p85β impacted p110α and p110β protein levels in PIK3CA mutant-only cells (Figure S3a), nor did overexpression of p85β affect the levels of p110α, p110β, and AKT phosphorylation in DLD1 PIK3CA E545K-only cells (Figure S3b). In contrast, overexpression of p85α increases the levels of p110α, p110β and AKT phosphorylation (Figure S3b). Those data suggest that p85α, but not p85β, is the major regulatory subunit for PI3K activity in DLD1 colorectal cancer cells.

It has been reported that p85 proteins can translocate to the nucleus [27-31]. We thus performed immunofluorescent staining of p85β in the isogenic DLD1 PIK3CA E545K-only and PIK3CA WT-only cell lines. As shown in Figure 3A, p85β was present in both nucleus and cytoplasm in the DLD1 PIK3CA E545K-only cells, but only in the cytoplasm in the DLD1 PIK3CA WT-only cells. The specificity of the anti-p85β antibody was demonstrated by the lack of staining in the DLD1 PIK3CA E545K-only p85β knockout cells (Figure 3a). Consistently, cell fractionation analyses showed that significantly more p85β was located in the nucleus in the DLD1 PIK3CA E545K-only cells than in the DLD1 PIK3CA WT-only cells (Figures 3b & 3c). In agreement with previous reports, a small fraction of p85α was also present in the nucleus (Figure 3b),

although the amounts of nuclear p85α were similar between the isogenic DLD1 PIK3CA E545K-only cells and DLD1 PIK3CA WT-only cells (Figure 3c). Because BRD7 was reported to facilitate nuclear translocation of p85α [27-31], we compared BRD7 protein levels between the DLD1 PIK3CA E545K-only and PIK3CA WT-only cells. Figure 3B shows that BRD7 proteins were largely localized to the nucleus to a similar degree in the two cell lines, suggesting that the differential nuclear localization of p85β in the DLD1 PIK3CA E545K cells is unlikely to be mediated by BRD7. Consistently, knockout of BRD7 in DLD1 cells largely abolished nuclear translocation of p85α but not p85β (Figures S3c and S3d).

To assess the generality and specificity of p85β nuclear localization in PIK3CA helical domain mutant cells, we analyzed cellular localization of p85β in a panel of cell lines: two additional PIK3CA E545K mutant cell lines (H460 and MB361); three PIK3CA H1047R mutant cells lines (HCT116, RKO, and T47D); and two WT PIK3CA cell lines (SW480 and LoVo). Both immunofluorescent staining and cell fractionation demonstrated that p85β was translocated into the nucleus in the cell lines with a PIK3CA E545K mutation, but not in cell lines with WT PIK3CA or H1047R mutation (Figures 3d to 3j). Furthermore, overexpressing PIK3CA E545K protein into SW480 cells facilitates the nuclear translocation of p85β (Figure S3e). Consistently, compared to PIK3CA wild-type tumors, immunohistochemistry staining of human colon cancer specimens showed that p85β was predominantly localized in the nuclei of tumors with a PIK3CA E545K mutation (Figure S3f), but mostly localized in the cytoplasm of tumors with wild-type PIK3CA (Figure S3g). Together, those data suggest that p85β dissociates from the PI3K complexes and translocates into the nucleus in cancer cells with a PIK3CA helical domain mutation.

Nuclear translocation of p85β is critical for tumorigenicity of PIK3CA E545K mutant cells.

To determine how p85β translocates into the nucleus, we exploited a nuclear localization sequence (NLS) prediction tool (cNLS Mapper) and identified a putative NLS at amino acids 474 to 484 of p85β (Figure 4a). To test if this NLS mediates nuclear translocation of p85β, we reconstituted the DLD1 PIK3CA E545K-only p85β KO cells with HA-tagged WT p85β, or mutant p85β construct, in which the two basic amino acids K477 and R478 in the NLS were mutated to alanine (Figure S4a). Although both the WT and K477A/R478A mutant p85β bound similarly to WT p110α and p110β, immunofluorescent staining and cell fractionation showed that the WT p85β translocated into the nucleus, but the K477A/R478A mutant p85β remained in the cytoplasm (Figures S4b & S4c). Interestingly, reconstitution of the WT, but not the mutant p85β, rescued the defects in cell growth and colony formation of the DLD1 PIK3CA E545K-only p85β KO cells (Figures S4d & S4e). As expected, both WT and the mutant p85β reduced their interactions with p110α E545K mutant protein, but retained the interactions with p110α H1047R mutant protein and p110β (Figures S4a & S4f). To further validate this observation, we generated p85β K477A/R478A mutant knockin (KI) DLD1 cells using CRISPR/Cas9 mediated gene editing (Figure 4b). Two independently-derived homozygous KI clones termed $p85\beta^{KR\text{-}AA}$ were chosen for in-depth analyses. The $p85\beta^{KR\text{-}AA}$ mutation did not impact levels of itself, p110α, p110β, and AKT phosphorylation (Figure 4c), suggesting that the p85β NLS mutant does not affect the kinase activity of PI3K. Nonetheless, the NLS mutant $p85\beta^{KR\text{-}AA}$ failed to translocate into the nucleus (Figure 4d). Moreover, $p85\beta^{KR\text{-}AA}$ mutant KI cell lines displayed reduced cell proliferation, colony formation, and xenograft tumor growth

(Figures 4e to 4g). Together, those data suggest that nuclear but not cytoplasmic p85β promotes the growth of cancer cells with a PIK3CA helical domain mutation.

Nuclear p85β stabilizes EZH1/2 proteins, thereby increasing H3K27 tri-methylation.

We postulated that the p85β present in the nucleus might regulate gene expression. Thus, we performed expression profiling of DLD1 parental cells and the two independently-derived $p85\beta^{KR-AA}$ mutant clones. Compared with the parental cells, expression levels of 137 genes were up-regulated, and 116 genes were down-regulated in both $p85\beta^{KR-AA}$ mutant clones (Figure S5a), suggesting that the nuclear p85β might regulate global gene transcription. We thus examined histone modifications in parental cells and $p85\beta^{KR-AA}$ mutant clones. As shown in Fig. 5A, levels of histone H3K27 trimethylation (H3K27me3) were reduced in the two $p85\beta^{KR-AA}$ mutant clones compared to the parental DLD1 cells (Figure 5a). Consistently, levels of H3K27me3 were higher in DLD1 PIK3CA E545K-only cells than in the isogenic PIK3CA WT-only cells (Figure 5b). Moreover, knockout of p85β in DLD1 PIK3CA E545K-only cells or knockdown of p85β in MB-361 cells, which harbors a PIK3CA E545K mutation, decreased the levels of H3K27me3 (Figure 5b). Conversely, the reconstitution of WT p85β, but not $p85\beta^{KR-AA}$ mutant, in DLD1 PIK3CA E545K-only p85β KO cells restored the levels of H3K27me3 (Figure 5c). In contrast, the depletion of p85β in DLD1 PIK3CA WT-only cells or T47D (PIK3CA H1047R mutant cells) had no impact on H3K27me3 (Figure 5b). Furthermore, knockout of p85β did not affect histone trimethylation at other sites, including H3K4, H3K9, H3K36, and H3K76 (Figure S5b). Taken together, the data suggest that nuclear p85β modulates H3K27me3, a marker for transcriptional repression.

Given that EZH1 and EZH2 are the histone methyltransferases for the H3K27 site, we next examined if nuclear p85β regulates EZH1 and EZH2. As shown in Figure 5A, compared to parental cells, levels of EZH1 and EZH2 proteins were markedly reduced in p85β^{KR-AA} mutant knockin clones. Consistently, levels of EZH1 and EZH2 proteins were higher in DLD1 PIK3CA E545K-only cells than in the isogenic PIK3CA WT-only cells (Figure 5b), whereas the depletion of p85β decreased EZH1 and EZH2 protein levels in PIK3CA E545K mutant cells (DLD1 E545K and MB-361), but not in cells with WT PIK3CA or a PIK3CA H1047R mutation (DLD1 PIK3CA WT and T47D) (Figure 5b). Conversely, the reconstitution of WT p85β, but not p85β^{KR-AA} mutant, in DLD1 PIK3CA E545K-only p85β KO cells restored EZH1 and EZH2 protein levels (Figure 5c). Moreover, the knockout of p85β reduced EZH 1 and EZH2 protein stability (Figure S5c). Consistently, the knockout of p85β in DLD1 PIK3CA E545K-only cells did not affect mRNA levels of EZH1 and EZH2 (Figure S5d). It is worth noting that the knockout of p85β did not impact other components of the PCR2 complex (Figure S5b). Together, these data suggest that nuclear p85β regulates EZH1 and EZH2 protein stability, thereby enhancing H3K27me3.

Nuclear p85β recruits USP7 to EZH1/2 to protect them from ubiquitin-mediated protein degradation.

We next set out to determine how nuclear p85β stabilizes EZH1 and EZH2 proteins. It has been reported that USP7 deubiquitinates and stabilizes EZH2 in prostate cancer cells [32,33]. We thus postulated that nuclear p85β brings USP7 to EZH1 and EZH2, thereby protecting them from ubiquitin-mediated protein degradation. This notion is supported by the following pieces of evidence: 1) immunoprecipitation analyses

showed that p85β interacted with USP7, EZH1, and EZH2 in DLD1 cells, which harbor a PIK3CA E545K mutation (Figure 5d); 2) more USP7 bound to EZH1 or EZH2 in DLD1 PIK3CA E545K-only cells than in the isogenic p85β KO cells (Figure 5e); 3) EZH1 and EZH2 protein levels were reduced in DLD1 USP7 KO cells that we generated previously [34], compared to the parental cells (Figure 5f); 4) proteasome inhibitor MG132 treatment restored EZH1 and EZH2 protein levels in USP7 KO cells (Figure 5g); and 5) EZH1 and EZH2 ubiquitination levels were increased in USP7 KO cells compared to the parental cells (Figure 5h). Moreover, the stabilization of EZH1 and EZH2 by the nuclear p85β seems not to involve the p110α or p110β catalytic subunits, because EZH1 and EZH2 bound to p85β, but not p110α and p110β (Figure S5e). Taken together, the data suggest that nuclear p85β recruits USP7 to stabilize EZH1/2, thereby enhancing H3K27 trimethylation.

A combination of an EZH inhibitor and the p110α inhibitor Alpelisib induces tumor repression.

We have shown that the nuclear p85β stabilizes EZH1 and EZH2 in cancer cells with a PIK3CA E545K mutation. Given that the mutation also activates p110α kinase activity, we hypothesized that a combination of an EZH inhibitor and a p110α inhibitor would have a better tumor inhibitory effect than either alone. We first tested a combination of p110α inhibitor Alpelisib (BYL-719) with an EZH inhibitor, GSK2816126. As shown in Figure 6A, the drug combination induced tumor regression of xenografts established from DLD1 cells, which harbor a PIK3CA E545K mutation, whereas single drugs alone only slowed tumor growth (Figure 6a). Similar results were obtained with a combination of Alpelisib with another EZH2 inhibitor Tazemetostat (Figure 6b). We chose Tazemetostat for in-depth studies, because it was recently approved by the FDA

to treat EZH2 mutant follicular lymphoma and advanced epithelioid sarcoma [35]. Our hypothesis predicts that tumors that harbor a PIK3CA helical domain mutation are more sensitive to the drug combination than tumors with WT PIK3CA. To test this notion, we treated tumors established from either PIK3CA E545K-only or PIK3CA WT-only cells. The combination of Alpelisib and Tazemetostat induced regression of tumors established with PIK3CA E545K-only (Fig. 6c), whereas the drug combination only slowed down the growth of the PIK3CA WT-only tumors (Fig. 6d). Moreover, the drug combination did not induce tumor regression of a CRC patient-derived xenograft (PDX) harboring a PIK3CA H1047R kinase domain mutation (Fig. 6e). As shown in Fig. 2, the PIK3CA helical domain mutations occurred in three residues (E545, E542, and Q546). Since we had demonstrated that the combination of Alpelisib and Tazemetostat induced tumor regression of PIK3CA E545K mutant tumors, we next tested if the drug combination induced regression of tumors harboring the other two recurrent PIK3CA helical domain mutations (E542K and Q546P). As shown in Figure 6 f and g, the combination of Alpelisib and Tazemetostat induced tumor regression of Vaco481 CRC cells with a PIK3CA Q546P mutation and a CRC PDX harboring a PIK3CA E542K mutation. As expected, compared to PIK3CA E542K mutant PDXs treated with vehicle control, Alpelisib reduced pAKT levels only, Tazemetostat reduced H3K27me3 only, whereas the drug combination decrease levels of both pAKT and H3K27me3 (Figure 6h). It is worth noting the drug combination was well-tolerated as the body weights of mice were maintained during the course of the drug treatments (Figure S6 a to h). These results suggest that the combination of Tezametostat and Alpelisib could be an effective treatment for cancers harboring PIK3CA helical domain mutations.

Discussion

Our study reveals a previously unrecognized mechanism by which PIK3CA helical domain mutations exert oncogenic signaling: p85β, but not p85α, dissociates from the p110α helical domain mutant protein and translocates into the nucleus. The nuclear p85β stabilizes EZH1/2 by recruiting deubiquitinase USP7 to the two proteins and enhancing H3K27 trimethylation. Additionally, our previous study demonstrated that the p110α helical domain mutant proteins directly bind to IRS1 and activate the canonical PDK1-AKT signaling pathways [12]. Therefore, PIK3CA helical domain mutations promote oncogenesis through two independent pathways: a canonical p110-PDK1-AKT pathway and a nuclear p85β-USP7-EZH1/2 axis (Figure 7). Moreover, our data suggest that targeting both pathways with Alpelisib and Tazemetostat could be an effective therapeutic approach for PIK3CA helical domain mutant cancers.

Firstly, this study sheds new light on the nuclear translocation and function of p85β. We identified an NLS (ELQMKRTAIEAF) in p85β that plays a major role in its nuclear translocation. When we mutated the critical basic amino acids KR to AA in both ectopically expressed and endogenous p85β, the mutant p85β protein fail to translocate into the nucleus (Figures 4 and S4). However, the p85β NLS is not sufficient to induce nuclear translocation, as our data showed that p85β translocates into the nucleus in the PIK3CA helical domain mutant cell lines, but not in the WT and PIK3CA kinase domain mutant cell lines (Figure 3). We postulate that the release of p85β from the PI3K complexes and exposure of the NLS in the iSH2 domain trigger p85β nuclear translocation. Although BRD7 has been reported to act as a chaperone for nuclear transport of p85α and p85β [30,31], our data suggest that BRD7 is not the major mediator

of p85β nuclear translocation in PIK3CA helical domain mutant cancer cells, because knockout of BRD7 only had a marginal effect on nuclear p85β levels. It is interesting that p85β, but not p85α, dissociates from the p110α helical domain mutant proteins. Our domain-swapping experiment shows that the N-terminal p85β sequences cause its dissociation from the p110α helical domain mutant proteins (Figure 1 i & j). Although p85α also has a putative NLS sequence, it still tightly binds to p110α helical mutant protein, which prevents it from the NLS-mediated nuclear translocation.

Secondly, our data suggest that the nuclear p85β plays an oncogenic role in tumors. Nuclear p85β has been shown to interact with XBP1 to modulate endoplasmic reticulum stress or binds to BRD7 and XBP1 to regulate glucose homeostasis [27-31,36]. Although it has been proposed that overexpression of p85β in some tumor types promotes cancer progression through the canonical PI3K enzymatic activity [22], none of the previous studies have implicated nuclear p85β in tumorigenesis. Here, we provide several lines of evidence implicating an oncogenic role of nuclear p85β in PIK3CA helical domain mutant cancers: (1) knockout of p85β reduces xenograft tumor growth of DLD1 PIK3CA E545K cells, but not the isogenic PIK3CA WT cells; (2) knockdown of p85β reduces the growth of a panel of PIK3CA helical domain mutant cell lines, not a panel of PIK3CA kinase domain mutant cell lines; (3) the p85β NLS mutant DLD1 knockin cells, lacking nuclear translocation of p85β, have reduced xenograft tumor growth.

Thirdly, our data suggest that the nuclear p85β stabilizes EZH1 and EZH2 by recruiting deubiquitinase USP7, and enhances H3K27 trimethylation, thereby promoting the growth of PIK3CA helical domain mutant tumors. Consistently, an oncogenic role of

EZH1/2, especially EZH2, has been well-documented because recurrent gain-of-function EZH2 mutations have been identified in 22% of diffuse large-cell B cell lymphomas and ~ 10% of follicular lymphomas [37]. Interestingly, the aforementioned oncogenic nuclear p85β function seems to be independent of p110α and p110β, because our data demonstrated that EZH1 and EZH2 bind to p85β, but not p110α and p110β (Fig. S5e).

Lastly, our data suggest that simultaneously targeting nuclear p85β-stabilized EZHs and p110α could be an effective cancer treatment. The p110α specific inhibitor Alpelisib in combination with Fulvestrant has been approved by the FDA for the treatment of HR-positive and HER2-negative breast cancers with PIK3CA mutation [38]. However, the efficacy of Alpelisib in other tumor types (such as colorectal cancer) has been disappointing [39]. Moreover, in some early clinical trials, patients with PIK3CA helical domain mutations are more resistant to Alpelisib than those with PIK3CA kinase domain mutations [16]. Thus, novel approaches are needed to target the PIK3CA helical domain mutations. Our data demonstrated that the combination of Alplelisb and EZH2 inhibitor Tazmetostat induced regression of tumors harboring each of the three recurrent PIK3CA helical domain mutations, but not tumors with PIK3CA WT or a kinase domain mutation. Currently, we have only tested the drug combination in CRC models. However, the molecular mechanisms we uncovered here apply to other types of tumor types with a PIK3CA helical domain mutation as well. Ultimately, the drug combination's efficacy needs to be tested in cancer patients. The FDA recently approved Alpelisib to treat PIK3CA-mutant, HER2-, and HR+ breast cancer patients, whereas Tazmetostat was just approved for EZH2 mutant follicular lymphoma and advanced epithelioid sarcoma. We are actively pursuing a phase I clinical trial of the combination

Alpelisib and Tazmetostat in patients whose tumors harbor a PIK3CA helical domain mutation.

Methods

Reagents

Chemicals, antibodies, and other reagents are listed in Table S1.

Tissue Culture and transfection

Colorectal cancer (CRC) cell lines DLD1, HCT116, RKO, SW480, LoVo, and genetically engineered isogenic cell lines DLD1 PIK3CA E545K cells and DLD1 PIK3CA WT cells were grown in McCoy's 5A medium (Gibco) supplemented with 10% of fetal bovine serum (Gibco). Lung cancer cell line H460 and breast cancer cell line T47D were cultured in RPMI 1640 medium (Sigma) containing 10% of FBS. Breast cancer cell line MDA-MB361 was maintained in Leibovitz's L-15 medium (Gibco) with 20% of FBS. Human embryonic kidney HEK 293T cells were cultured in DMEM medium (Sigma) containing 10% FBS. Penicillin/Streptomycin (1%) was added to tissue culture media for all cultures. Cells were incubated at 37 ℃ in a humidified atmosphere with 5% CO_2. All cell lines were tested routinely to avoid *Mycoplasma* contamination (Yeasen, cat # 40601ES20). The cell lines were authenticated by the Genetica DNA Laboratories using STR profiling. Transfection was conducted using Lipofectamine 3000 reagent (Life Technologies) according to the manufacturer's instructions.

DNA constructs and mutagenesis

The plasmids we constructed in this study are listed in Table S1. The primers which were used for vector construction are listed in Table S2. Briefly, pCMV backbones (Invitrogen) were used for gene expression in mammalian cells using the USER cloning system [40]. LentiCRISPR V2 backbone (Addgene) was used for gene knockout in cells. Point mutations in constructs were generated using a Site-Directed Mutagenesis Kit (Agilent). pAAV-loxP-Neo vector was used for homologous recombination of endogenous p85β NLS point mutation.

CRISPR/CAS9 genome editing

Three different guiding RNA pairs for p85βknockout were designed using the IDT design tool (https://sg.idtdna.com/pages) and cloned individually into the lentiCRISPRv2 vector as described previously [41]. DLD1 isogenic cell lines with PIK3CA E545K or with wild-type PIK3CA were transfected with these vectors. After 48 hours, cells were trypsinized, and stable clones were selected using 1.5 μg/ml puromycin (Invitrogen) for 2 weeks. Knock-out of p85β was screened using genomic PCR and validated by Western blot.

For CRISPR/CAS9 mediated NLS point mutation on endogenous PIK3R2 locus, 3 different guide RNA pairs surrounding NLS mutation sites of PIK3R2 locus were designed and cloned. Homologous arms of the NLS target sites were mutated and cloned into the pAAV-loxP-Neo vector. Targeting vectors were co-transfected with individual gRNA vectors into DLD1 cells. p85β NLS mutated cell clones were screened by genomic PCR and verified by genomic DNA sequencing.

siRNA knockdown

The siRNAs targeting human PIK3R2/p85β and the scramble siRNA control were purchased from Biotend (Shanghai, China). siRNAs were performed as described previously [34]. Cells were harvested 48-72 hours post-transfection for various assays.

RNA extraction and Quantitative Real-Time PCR

Total RNA was extracted and purified using TRIzol (Invitrogen) according to the manufacturer's instructions, and 1 μg of total RNA was reverse transcribed using the PrimeScript RT Reagent Kit (TaKaRa, Japan). The gene expression levels were measured by a quantitative real-time PCR system (Qiagen, Germany). β-tubulin was used as the reference gene for normalization. The qRT-PCR primers were listed in Table S2.

Cell growth assays

For cell proliferation, 3000 cells per well were seeded in a 96-well plate. Cell viability was measured for 5 consecutive days using Cell Counting Kit-8 (Dojindo, Japan) according to the manufacturer's instructions. Absorbance at OD450 was used to plot cell growth curves. For clone formation assay, the same number of cells were seeded in 6-well plates and maintained in McCoy's 5A medium with 1% FBS. After 14 days, cells were washed with PBS and stained with 0.5% crystal violet.

Immunofluorescence staining

Immunofluorescence staining was performed as described previously [42]. Briefly, cells were seeded on coverslips in a 6-well plate. After 24 to 48 hours, cells were fixed in 4% paraformaldehyde for 20 min, permeabilized with 0.5% Triton X-100 for 30 min, and blocked in 10% goat serum for 1 hour at room temperature. The cells were then

incubated with p85β antibodies in 10% goat serum at 4℃ overnight, followed by incubation with secondary fluorochrome-labeled antibodies for 40 min at 37 ℃. After incubation with DAPI for 3-5 min at room temperature to stain the nucleus, cells were washed three times with PBS and imaged with a confocal laser scanning microscope.

Co-immunoprecipitation and Western blotting

Co-immunoprecipitation (Co-IP) was performed as previously described[43]. For transfection-based Co-IP assays, cells were transfected with indicated vectors and lysed in 1 mL of lysis buffer (50 mM Tris-HCl at pH 7.5, 1 mM EDTA at pH 8.0, 150 mM NaCl, 1% NP-40, cOmplete Protease Inhibitor, PhosSTOP, and PMSF). Cell lysates were immunoprecipitated with indicated primary antibodies overnight at 4℃ and then Protein A/G for 2 hrs. The beads were washed three times with the lysis buffer and eluted in SDS sample buffer. The eluted immunocomplexes were resolved by SDS-PAGE, followed by Western blotting.

Nuclear/cytoplasmic fractionation

Cell pellets were resuspended in 1 ml fractionation buffer (0.1% NP-40, cOmplete Protease Inhibitor, PhosSTOP, and PMSF in PBS buffer) and gently pipetted up and down 15 times and then centrifuged at 12000 rpm for 30 seconds immediately. The supernatants were labeled as cytoplasmic fractions. The pellets were washed twice with fractionation buffer and then dissolved in 160 μl of fractionation buffer as the nuclear fraction. Each fraction was sonicated 10 seconds at 60% output settings.

Xenografts

All animal experiments were performed in accordance with protocols approved by

either the IACUC committee at Case Western Reserve University. Xenografts were established as described previously [44]. Briefly, for cells, three million cells were injected subcutaneously and bilaterally into athymic nude mice. For PDXs, two pieces of xenograft tumors (~2 to 4 mm^3) were inserted subcutaneously and bilaterally into athymic nude mice. Tumor volume was measured at the indicated time points and calculated as length×$width^2$/2.

Drug treatment

Alpelisib (BYL719) and Tazematostat (EPZ-6438) were dissolved in 0.5% carboxymethylcellulose sodium salt (CMC). GSK2816126 was dissolved in 20% Captisol. Once tumor sizes reached 100-150 mm^3, mice were randomly assigned into different groups (5 mice per group) and treated with vehicle, Alpelisib (BYL719, 12.5mg/kg, oral gavage, once daily), EPZ-6438 [500 mg/kg, oral gavage, bid as described in [45]], GSK2816126 (25mg/kg, once daily, I.P.), a combination of BYL719 and EPZ-6438, or a combination of BYL719 and GSK2816126.

Microarray analysis

DLD1 cells and two independently-derived clones of DLD1 $p85^{KR-AA}$ mutant cells were grown to 80% confluence in 6-well plates, and RNAs were extracted for microarray analysis. Input RNA was provided at 50 ng/ul, and the labeling reaction was initiated with 150 ng of RNA. Protocol for the chemistry used to prepare the samples for interrogation on the expression microarrays followed the manufacturer's instructions. Samples were labeled robotically using the Affymetrix WT [Whole transcript] labeling protocol and the Beckman Coulter Biomek® FX^P Laboratory Automation Workstation; scripts were provided by Affymetrix to process up to 96 samples in batch. Samples were

interrogated on the Human Gene Array 2.1 in the PEG format. Hybridization, washing, staining, and data collection were carried out in the Affymetrix Gene Titan MC [Multi channel] instrument. Differential expression of genes (DLD1 vs. both $p85^{KR-AA}$ Mut clones, fold change ≥ 2 or ≤ -2 and p-value ≤ 0.05) was analyzed by the Gene Expression and Genotyping Facility of Case Western Reserve University.

Immunohistochemistry

Immunohistochemistry was performed as described previously [46,47]. Briefly, paraffin-embedded mouse and human tissues were deparaffinized in xylene and antigen retrieved by boiling the sample for 20 min. Samples were incubated with primary antibodies at 4 °C overnight. The sections were stained with secondary antibody for 30 min at room temperature and then stained with an EnVision-HRP kit (Dako).

Mining the TCGA datasets

The dataset files of colorectal cancer (COAD), bladder carcinoma (BLCA), endometrial carcinoma (UCEC), and breast cancer (BRCA) were downloaded from the TCGA website. The files include the RNA-seq files providing normalized FPKM values, the somatic mutations, and the 5-year survival of each patient.

For gene expression analysis, FPKM values of indicated genes from tumor samples and corresponding normal tissue samples, if available, were plotted. The statistical significance difference of tumor versus non-tumor was calculated using the student t-test.

To analyze the association of PIK3R2 expression with 5-year survival, patients were

divided into three groups according to their PIK3CA mutation status: helical domain mutation group (Patients with PIK3CA mutation at E542, E545, and Q546), non-helical domain mutation group (Patients with PIK3CA mutation at H1047 and other sites) and wild type group (Patients with wild-type PIK3CA), and then patients were further divided into PIK3R2 high and PIK3R2 low according to the median expression of PIK3R2 in each group. Due to the limitation of the patient number of helical domain mutation group in individual tumor type, PIK3R2 high and PIK3R2 low in each group of four tumor types were combined to assess the relevance of PIK3R2 expression and 5-year survival of all patients. Kaplan-Meier analysis of 5-year survival was performed with a Cox proportional hazards model.

QUANTIFICATION AND STATISTICAL ANALYSIS

GraphPad Prism software was used to create the graphs. Data are plotted as mean $\pm$ SEM. We applied the *t*-test to compare the means between the two groups, assuming unequal variances. For xenograft growth, we carried out ANOVA for repeated measurements to test whether there is an overall difference in the tumor sizes by testing group differences as well as whether there was a difference in the development of tumor sizes over time between the 2 groups by testing the interaction between time and group.

List of Supplementary Materials:

Supplementary Figures 1 to 7.

Table S1: List of reagents.

Table S2: List of primers.

References:

1 Samuels, Y. *et al.* High frequency of mutations of the PIK3CA gene in human cancers. *Science* **304**, 554, doi:10.1126/science.1096502 [pii] (2004).

2 Saal, L. H. *et al.* PIK3CA mutations correlate with hormone receptors, node metastasis, and ERBB2, and are mutually exclusive with PTEN loss in human breast carcinoma. *Cancer research* **65**, 2554-2559 (2005).

3 Kandoth, C. *et al.* Mutational landscape and significance across 12 major cancer types. *Nature* **502**, 333-339, doi:10.1038/nature12634 (2013).

4 Markham, A. Alpelisib: First Global Approval. *Drugs* **79**, 1249-1253, doi:10.1007/s40265-019-01161-6 (2019).

5 Cantley, L. C. The phosphoinositide 3-kinase pathway. *Science* **296**, 1655-1657, doi:10.1126/science.296.5573(2002).

6 Vadas, O., Burke, J. E., Zhang, X., Berndt, A. & Williams, R. L. Structural basis for activation and inhibition of class I phosphoinositide 3-kinases. *Science signaling* **4**, doi:10.1126/scisignal.2002165 re2(2011).

7 Hao, Y., Zhao, S. & Wang, Z. Targeting the protein-protein interaction between IRS1 and mutant p110alpha for cancer therapy. *Toxicologic pathology* **42**, 140-147, doi:10.1177/0192623313506794 (2014).

8 Miled, N. *et al.* Mechanism of two classes of cancer mutations in the phosphoinositide 3-kinase catalytic subunit. *Science* **317**, 239-242, doi:10.1126/science.1135394 (2007).

9 Huang, C. H. *et al.* The structure of a human p110alpha/p85alpha complex elucidates the effects of oncogenic PI3Kalpha mutations. *Science* **318**, 1744-1748, doi:10.1126/science.1150799 (2007).

10 Carson, J. D. *et al.* Effects of oncogenic p110alpha subunit mutations on the lipid kinase activity of phosphoinositide 3-kinase. *The Biochemical journal* **409**, 519-524, doi:BJ20070681 [pii]10.1042/BJ20070681 (2008).

11 Burke, J. E., Perisic, O., Masson, G. R., Vadas, O. & Williams, R. L. Oncogenic mutations mimic and enhance dynamic events in the natural activation of phosphoinositide 3-kinase p110alpha (PIK3CA). *Proceedings of the National Academy of Sciences of the United States of America* **109**, 15259-15264, doi:1205508109 [pii]10.1073/pnas.1205508109 (2012).

12 Hao, Y. *et al.* Gain of interaction with IRS1 by p110alpha-helical domain mutants is crucial for their oncogenic functions. *Cancer Cell* **23**, 583-593, doi:10.1016/j.ccr.2013.03.021 S1535-6108(13)00129-3 [pii] (2013).

13 Zhao, L. & Vogt, P. K. Helical domain and kinase domain mutations in p110alpha of phosphatidylinositol 3-kinase induce gain of function by different mechanisms. *Proceedings of the National Academy of Sciences of the United States of America* **105**, 2652-2657, doi:0712169105 [pii]10.1073/pnas.0712169105 (2008).

14 Pang, H. *et al.* Differential enhancement of breast cancer cell motility and metastasis by helical and kinase domain mutations of class IA phosphoinositide 3-kinase. *Cancer research* **69**, 8868-8876, doi:0008-5472.CAN-09-1968 [pii]10.1158/0008-5472.CAN-09-1968 (2009).

15 Janku, F. *et al.* PIK3CA mutation H1047R is associated with response to PI3K/AKT/mTOR signaling pathway inhibitors in early-phase clinical trials. *Cancer research* **73**, 276-284, doi:10.1158/0008-5472.CAN-12-1726 (2013).

16 Mayer, I. A. *et al.* A Phase Ib Study of Alpelisib (BYL719), a PI3Kalpha-Specific Inhibitor, with Letrozole in ER+/HER2- Metastatic Breast Cancer.

Clinical cancer research : an official journal of the American Association for Cancer Research **23**, 26-34, doi:10.1158/1078-0432.CCR-16-0134 (2017).

17 Vallejo-Diaz, J., Chagoyen, M., Olazabal-Moran, M., Gonzalez-Garcia, A. & Carrera, A. C. The Opposing Roles of PIK3R1/p85alpha and PIK3R2/p85beta in Cancer. *Trends in cancer* **5**, 233-244, doi:10.1016/j.trecan.2019.02.009 (2019).

18 Cheung, L. W. *et al.* High frequency of PIK3R1 and PIK3R2 mutations in endometrial cancer elucidates a novel mechanism for regulation of PTEN protein stability. *Cancer discovery* **1**, 170-185, doi:10.1158/2159-8290.CD-11-0039 (2011).

19 Quayle, S. N. *et al.* Somatic mutations of PIK3R1 promote gliomagenesis. *PLoS One* **7**, e49466, doi:10.1371/journal.pone.0049466 PONE-D-12-21915 [pii] (2012).

20 Taniguchi, C. M. *et al.* The phosphoinositide 3-kinase regulatory subunit p85alpha can exert tumor suppressor properties through negative regulation of growth factor signaling. *Cancer research* **70**, 5305-5315, doi:10.1158/0008-5472.CAN-09-3399 (2010).

21 Thorpe, L. M. *et al.* PI3K-p110alpha mediates the oncogenic activity induced by loss of the novel tumor suppressor PI3K-p85alpha. *Proceedings of the National Academy of Sciences of the United States of America* **114**, 7095-7100, doi:10.1073/pnas.1704706114 (2017).

22 Cortes, I. *et al.* p85beta phosphoinositide 3-kinase subunit regulates tumor progression. *Proc Natl Acad Sci U S A* **109**, 11318-11323, doi:10.1073/pnas.1118138109 (2012).

23 Vallejo-Diaz, J. *et al.* Targeted depletion of PIK3R2 induces regression of lung squamous cell carcinoma. *Oncotarget* **7**, 85063-85078, doi:10.18632/oncotarget.13195 (2016).

24 Cariaga-Martinez, A. E. *et al.* Phosphoinositide 3-kinase p85beta regulates invadopodium formation. *Biology open* **3**, 924-936, doi:10.1242/bio.20148185 (2014).

25 Ito, Y., Hart, J. R., Ueno, L. & Vogt, P. K. Oncogenic activity of the regulatory subunit p85beta of phosphatidylinositol 3-kinase (PI3K). *Proceedings of the National Academy of Sciences of the United States of America* **111**, 16826-16829, doi:10.1073/pnas.1420281111 (2014).

26 Ito, Y., Vogt, P. K. & Hart, J. R. Domain analysis reveals striking functional differences between the regulatory subunits of phosphatidylinositol 3-kinase (PI3K), p85alpha and p85beta. *Oncotarget* **8**, 55863-55876, doi:10.18632/oncotarget.19866 (2017).

27 Winnay, J. N., Boucher, J., Mori, M. A., Ueki, K. & Kahn, C. R. A regulatory subunit of phosphoinositide 3-kinase increases the nuclear accumulation of X-box-binding protein-1 to modulate the unfolded protein response. *Nature medicine* **16**, 438-445, doi:10.1038/nm.2121 (2010).

28 Park, S. W. *et al.* The regulatory subunits of PI3K, p85alpha and p85beta, interact with XBP-1 and increase its nuclear translocation. *Nature medicine* **16**, 429-437, doi:10.1038/nm.2099 (2010).

29 Madhusudhan, T. *et al.* Defective podocyte insulin signalling through p85-XBP1 promotes ATF6-dependent maladaptive ER-stress response in diabetic nephropathy. *Nature communications* **6**, 6496, doi:10.1038/ncomms7496 (2015).

30 Park, S. W. *et al.* BRD7 regulates XBP1s' activity and glucose homeostasis

through its interaction with the regulatory subunits of PI3K. *Cell metabolism* **20**, 73-84, doi:10.1016/j.cmet.2014.04.006 (2014).
31 Chiu, Y. H., Lee, J. Y. & Cantley, L. C. BRD7, a tumor suppressor, interacts with p85alpha and regulates PI3K activity. *Molecular cell* **54**, 193-202, doi:10.1016/j.molcel.2014.02.016 (2014).
32 Lee, J. E., Park, C. M. & Kim, J. H. USP7 deubiquitinates and stabilizes EZH2 in prostate cancer cells. *Genet Mol Biol* **43**, e20190338, doi:10.1590/1678-4685-GMB-2019-0338 (2020).
33 Zheng, N., Chu, M., Lin, M., He, Y. & Wang, Z. USP7 stabilizes EZH2 and enhances cancer malignant progression. *American journal of cancer research* **10**, 299-313 (2020).
34 Du, Z. *et al.* DNMT1 stability is regulated by proteins coordinating deubiquitination and acetylation-driven ubiquitination. *Science signaling* **3**, ra80, doi:3/146/ra80 [pii] 10.1126/scisignal.2001462 (2010).
35 Rothbart, S. B. & Baylin, S. B. Epigenetic Therapy for Epithelioid Sarcoma. *Cell* **181**, 211, doi:10.1016/j.cell.2020.03.042 (2020).
36 Kumar, A. *et al.* Nuclear but not cytosolic phosphoinositide 3-kinase beta has an essential function in cell survival. *Molecular and cellular biology* **31**, 2122-2133, doi:10.1128/MCB.01313-10 (2011).
37 Kim, K. H. & Roberts, C. W. Targeting EZH2 in cancer. *Nature medicine* **22**, 128-134, doi:10.1038/nm.4036 (2016).
38 Andre, F. *et al.* Alpelisib for PIK3CA-Mutated, Hormone Receptor-Positive Advanced Breast Cancer. *The New England journal of medicine* **380**, 1929-1940, doi:10.1056/NEJMoa1813904 (2019).
39 Juric, D. *et al.* Phosphatidylinositol 3-Kinase alpha-Selective Inhibition With Alpelisib (BYL719) in PIK3CA-Altered Solid Tumors: Results From the First-in-Human Study. *Journal of clinical oncology : official journal of the American Society of Clinical Oncology* **36**, 1291-1299, doi:10.1200/JCO.2017.72.7107 (2018).
40 Zhang, X. *et al.* Epitope tagging of endogenous proteins for genome-wide ChIP-chip studies. *Nat Methods* **5**, 163-165, doi:nmeth1170 [pii]10.1038/nmeth1170 (2008).
41 Zhao, Y. *et al.* 5-Fluorouracil Enhances the Antitumor Activity of the Glutaminase Inhibitor CB-839 against PIK3CA-Mutant Colorectal Cancers. *Cancer research* **80**, 4815-4827, doi:10.1158/0008-5472.CAN-20-0600 (2020).
42 Zhang, X. *et al.* Identification of STAT3 as a substrate of receptor protein tyrosine phosphatase T. *PNAS* **104**, 4060-4064, doi:10.1073/pnas.0611665104 (2007).
43 Hao, Y. *et al.* Oncogenic PIK3CA mutations reprogram glutamine metabolism in colorectal cancer. *Nature communications* **7**, 11971, doi:10.1038/ncomms11971 (2016).
44 Zhao, Y. *et al.* Colorectal cancers utilize glutamine as an anaplerotic substrate of the TCA cycle in vivo. *Sci Rep* **9**, 19180, doi:10.1038/s41598-019-55718-2 (2019).
45 Knutson, S. K. *et al.* Durable tumor regression in genetically altered malignant rhabdoid tumors by inhibition of methyltransferase EZH2. *Proceedings of the National Academy of Sciences of the United States of America* **110**, 7922-7927, doi:10.1073/pnas.1303800110 (2013).
46 Zhao, Y. *et al.* Identification and functional characterization of paxillin as a

target of protein tyrosine phosphatase receptor T. *Proceedings of the National Academy of Sciences of the United States of America* **107**, 2592-2597, doi:10.1073/pnas.0914884107 (2010).
47 Zhao, Y. *et al.* Regulation of paxillin-p130-PI3K-AKT signaling axis by Src and PTPRT impacts colon tumorigenesis. *Oncotarget* **8**, 48782-48793, doi:10.18632/oncotarget.10654 (2017).

Acknowledgment:

This work was supported by NIH grants R01CA196643, R01CA264320, P50CA150964, and a Stand Up to Cancer Colorectal Cancer Dream Team Translational Research Grant (SU2C-AACR-DT22-17) to Z. Wang. Stand Up to Cancer is a program of the Entertainment Industry Foundation. Research grants are administered by the American Association for Cancer Research, a scientific partner of SU2C. This work was also supported by the Program for Professor of Special Appointment (Eastern Scholar) at Shanghai Institutions of Higher Learning (TP2017027); the Program of Shanghai Academic/Technology Research Leader (19XD1423500); Shanghai Municipal Education Commission-Gaofeng Clinical Medicine Grant Support (20171915); National Natural Science Foundation of China (81772503, 82073044); and State Key Laboratory of Oncogenes and Related Gene (91-17-10, ZZ2016SYL) to Y. Hao. This research was further supported by the Gene Expression and Genotyping Facility of the Case Comprehensive Cancer Center (P30 CA043703) directed by M. Veigl.

Author contributions

ZW and YH conceived the experiments. YH, BH, LW, YL, CW, TW, Y. Zhang, LS, Y. Zhan, Y. Zhao and MV performed the experiments and analyzed the data. SM provided essential reagents. ZW, YH, RC and BH wrote the manuscript.

Conflict of Interest

The authors declare no conflict of interest.

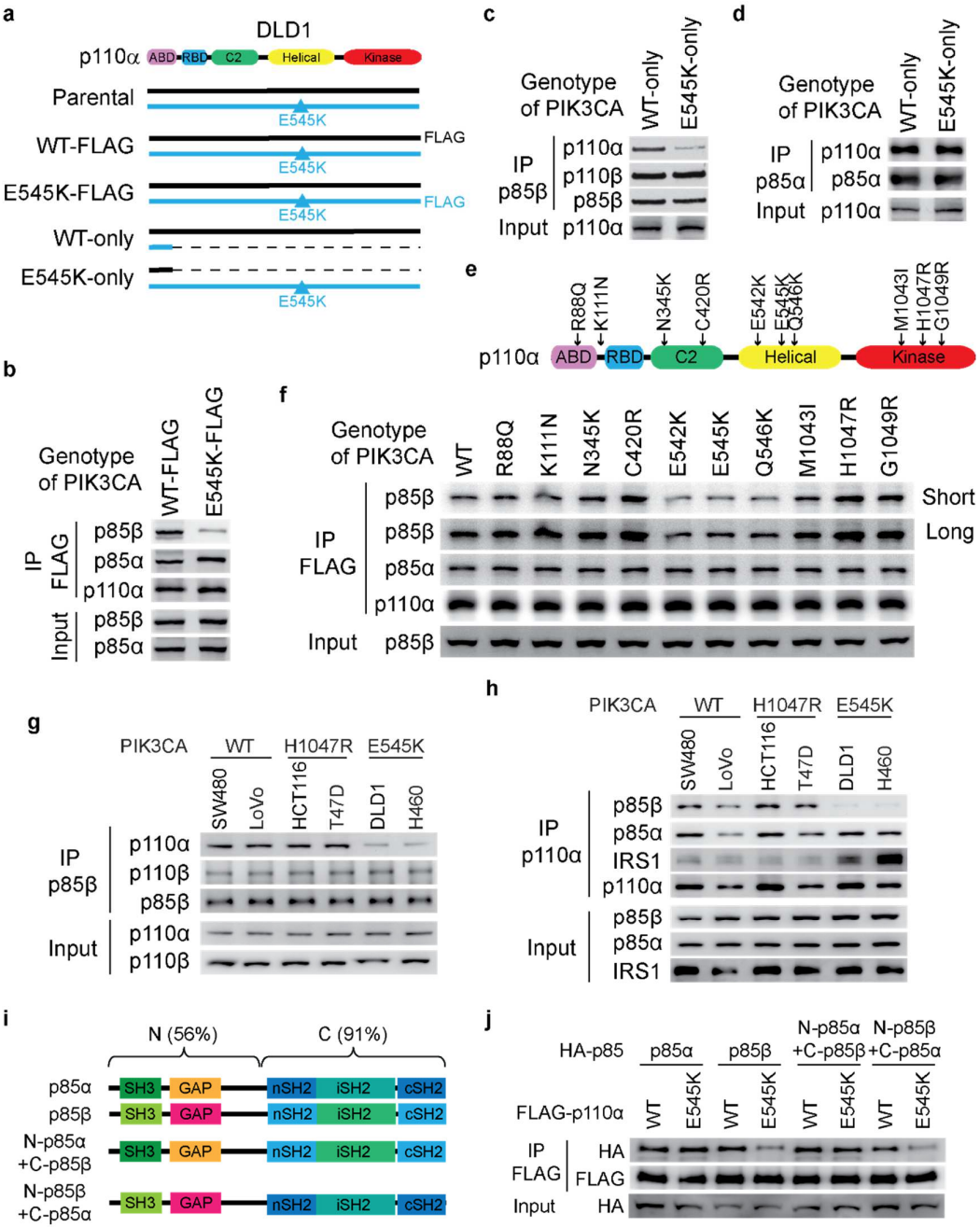

Figure 1. p85β disassociates from the p110α helical domain-mutant protein.

(a) Schematic of DLD1 isogenic cell lines. WT-FLAG: DLD1 cells with the endogenous wild-type p110α tagged with 3×FLAG; E545K-FLAG: DLD1 cells with the endogenous p110α E545K mutant protein tagged with 3×FLAG; WT-only: DLD1 cells with the PIK3CA E545K allele knocked out; E545K-only: DLD1 cells with the PIK3CA WT allele knocked out. ABD: adaptor-binding domain; RBD: Ras-binding domain; C2: C2 domain; helical: helical domain; kinase: kinase domain.

(b-d) p85β, but not p85α, disassociates from p110α E545K mutant protein. Cell lysates from the p110α E545K or WT FLAG-tagged cells were immunoprecipitated with anti-FLAG antibody-conjugated beads and blotted with indicated antibodies (b). Cell lysates from the indicated cell lines were immunoprecipitated with either an anti-p85β antibody (c) or an anti-p85α antibody (d) and blotted with indicated antibodies.

(e) A schematic diagram of tumor-derived PIK3CA mutations tested for interaction with p85β.
(f) p85β, but not p85α, disassociates from p110α helical domain mutant proteins. The indicated FLAG-tagged p110α constructs were transfected into 293T cells. Cell lysates were immunoprecipitated by anti-FLAG agarose and then blotted with the indicated antibodies.
(g & h) p85β disassociates from PI3K complexes in PIK3CA helical domain mutant cells. Cell lysates from indicated cell lines were immunoprecipitated with either an anti-p85β antibody (G) or an anti-p110α antibody (H) and blotted with indicated antibodies.
(**i & j**) The N-terminal domains of p85β cause disassociation from p110α E545K mutant protein. Schematics of p85α, p85β and two chimeric p85 constructs (I). The indicated HA-tagged p85 constructs were co-transfected with a Flag-tagged construct expressing either WT or E545K mutant p110α. Cell lysates were immunoprecipitated by anti-FLAG agarose and then blotted with an anti-HA antibody.

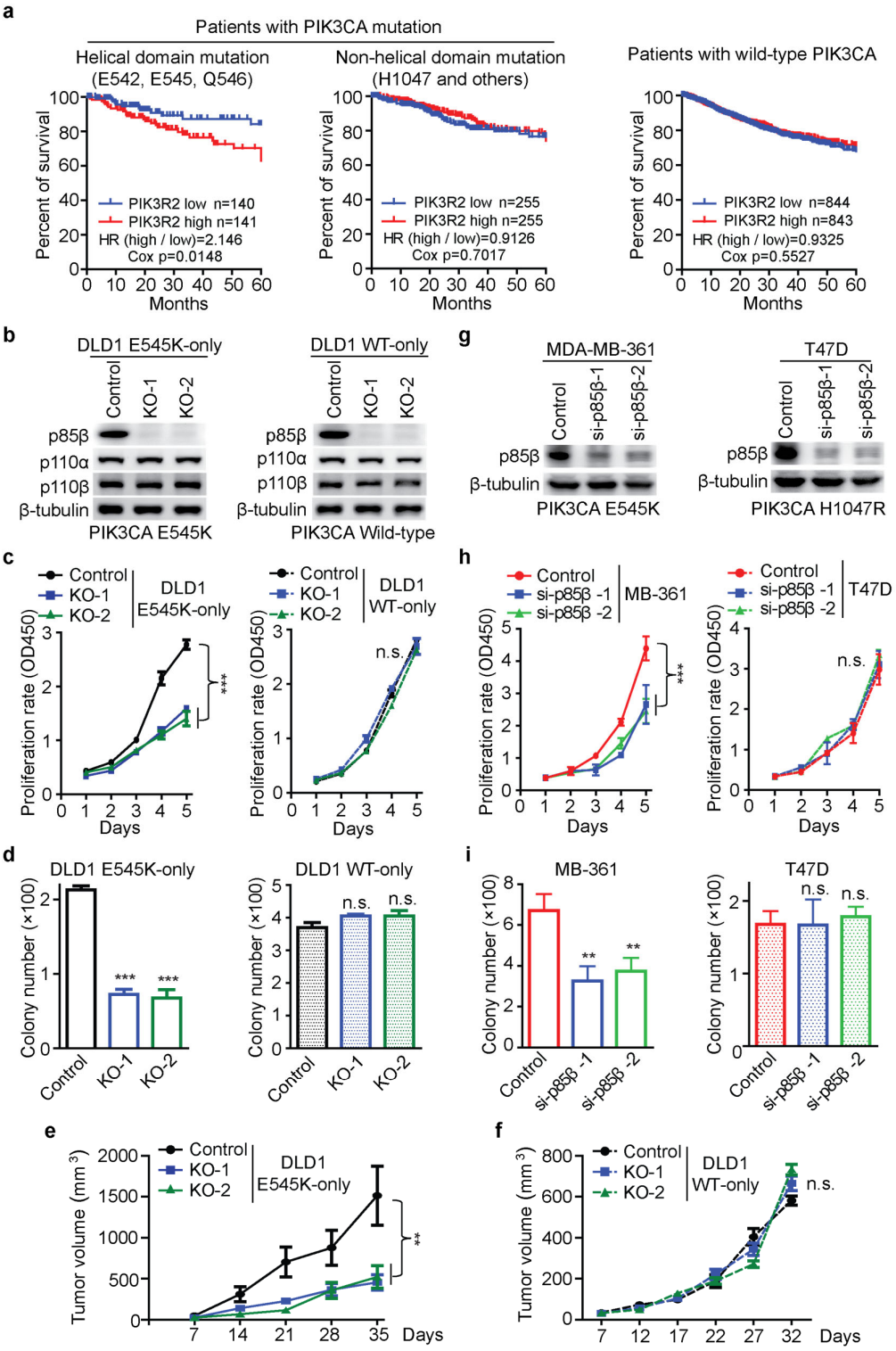

Figure 2. p85β plays an oncogenic role in cancer cells with PIK3CA helical domain mutations.

(a) High levels of PIK3R2 (p85ß) are associated with worse survival of patients whose tumors harbor a PIK3CA helical domain mutation. COAD, BLCA, UCEC, and BRAC datasets were downloaded from TGCA and combined. Patients were divided into three groups according to their PIK3CA mutation status: Helical domain mutations, Non-

helical domain mutations, and wild-type. Kaplan-Meier analyses of 5-year survival of patients whose tumors expressing high levels of PIK3R2 *vs* low levels of PIK3R2 were performed. HR: Hazard Ratio.

(b-f) Knockout of p85β impairs the growth of cancer cells with a PIK3CA E545K mutation, but not cells with WT PIK3CA. PIK3R2 (p85β) was knocked out in the indicated cell lines, and the cells were assayed for: Western blot analyses of p85β, p110α and p110 β proteins (b); cell proliferation (c); colony formation (d); and xenograft tumor growth (e & f).

(g-j) Depletion of p85β impairs the growth of cancer cells with a PIK3CA E545K mutation, but not cells with a PIK3CA H1047R mutation. p85β was knocked down with two independent siRNAs in the indicated cell lines, and the cells were assayed for: Western blot analyses of p85β protein (g); cell proliferation (h); colony formation (i).

Statistical analyses, two-way ANOVA was used for c, e, f & h, and student's *t*-test was used for d & i. Data are presented as mean ± SEM of three independent experiments. ** $p < 0.01$; *** $p < 0.001$; n.s., not significant.

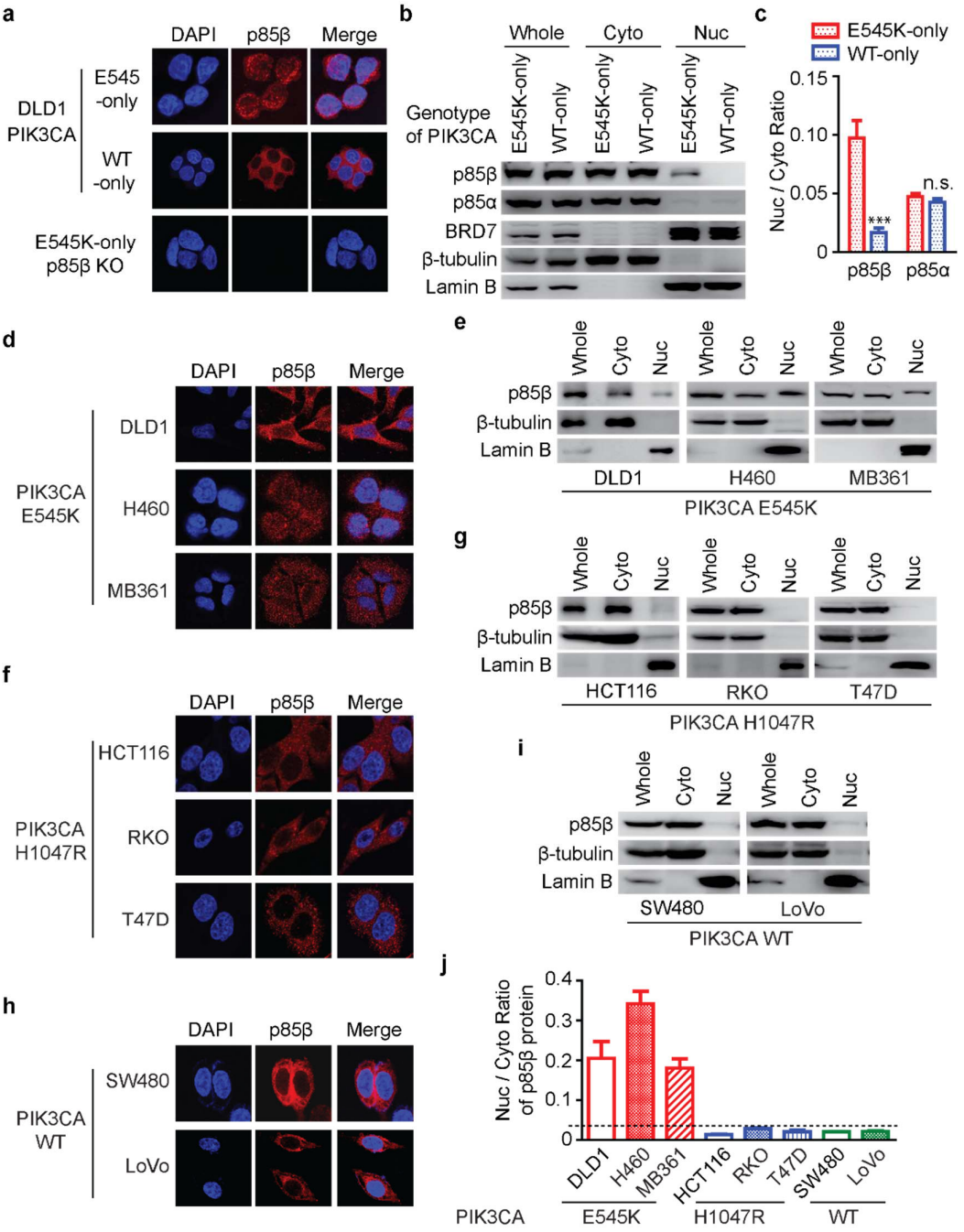

Figure 3. p85β translocates into the nucleus in cancer cells with a PIK3CA E545K mutation.

(a-c) p85β translocates into the nucleus in DLD1 PIK3CA E545K cells. (a) The indicated cells were immunofluorescently stained with an anti-p85β antibody and DAPI. (b) Cell lysates were fractionated into cytoplasmic (Cyto) and nuclear (Nuc) fractions and blotted with the indicated antibodies. Whole: whole cell lysate. The ratios of nuclear/cytoplasmic p85β levels were quantified by Image J as shown in (c). Data are presented as mean ± SEM of three independent experiments. *** $p < 0.001$; n.s., not significant.

(d-j) p85β translocates into the nucleus in cancer cells with a PIK3CA helical domain mutation, but not cells with WT PIK3CA or a PIK3CA kinase domain mutation. The

indicated cells were immunofluorescently stained with an anti-p85β antibody, and representative images are shown in (d), (f), and (h). Cell lysates of the indicated cells were fractionated into cytoplasmic and nuclear fractions and blotted with the indicated antibodies (e), (g), and (i). The ratios of nuclear/cytoplasmic p85β levels were quantified by Image J and shown in (j). Data are presented as mean ± SEM of three independent experiments.

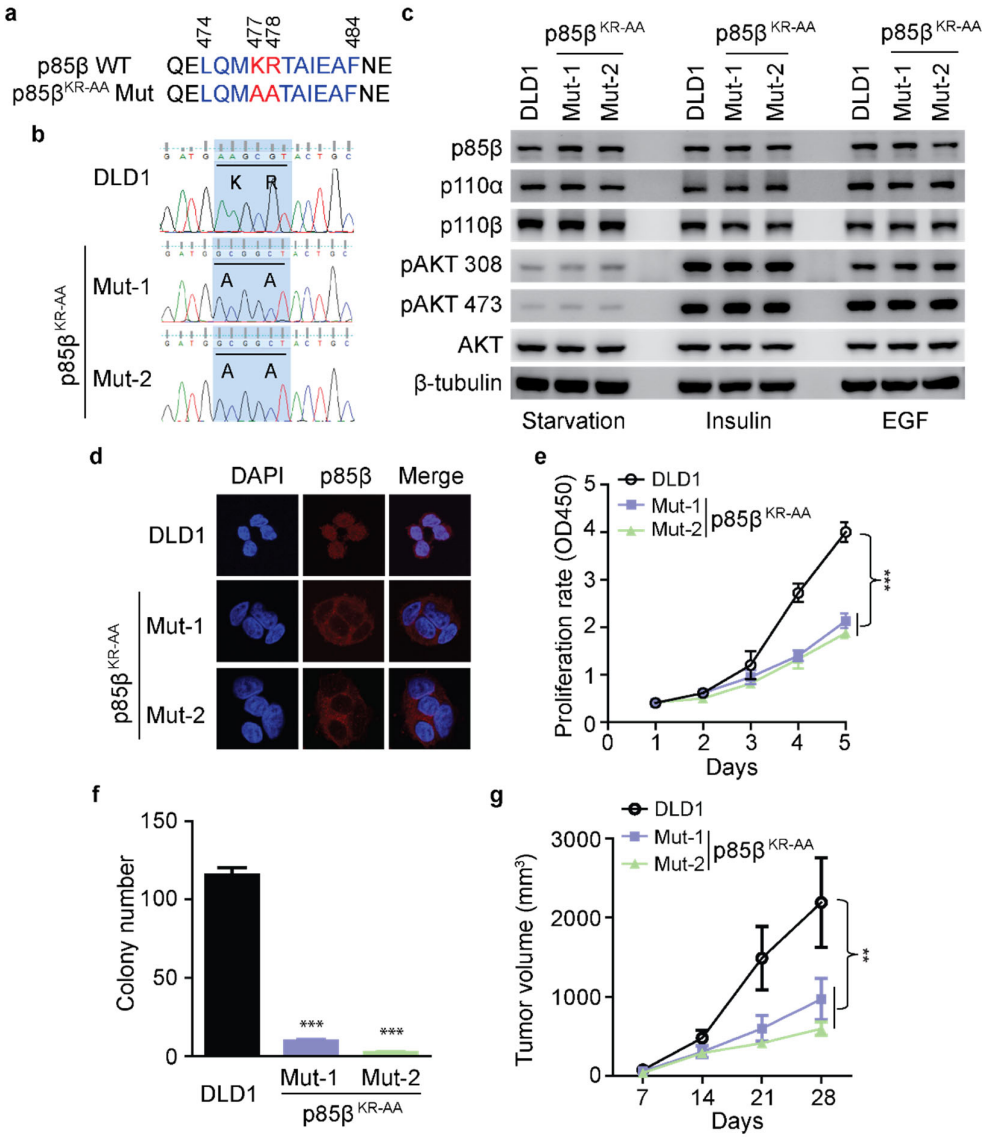

Figure 4. Nuclear translocation of p85β is critical for the tumorigenicity of PIK3CA E545K mutant cells.

(a) A predicted Nuclear Localization Sequence (NLS) in p85β protein is highlighted in blue. The critical stretch basic amino acids $K^{477}R^{478}$ are highlighted in red.

(b) Genomic DNA sequencing of DLD1 parental cells and $K^{477}A$ $R^{478}A$ mutant knock-in ($p85\beta^{KR-AA}$) cells.

(c) NLS mutation has no impact on p85β, p110α and p110β protein levels and AKT phosphorylation. Cells of the indicated genotypes were serum-starved, stimulated with insulin or EGF, and then lysed and blotted with indicated antibodies.

(d) Cells of the indicated genotype were stained with an anti-p85β antibody. Mut-1 and Mut-2 are two independently derived $p85\beta^{KR-AA}$ mutant knock-in clones.

(e-g) Cells of the indicated genotypes were assayed for cell proliferation (e), colony formation (f), and xenograft tumor growth (g).

Statistical analyses, two-way ANOVA was used for e & g, and student's *t*-test was used for f. Data are presented as mean ± SEM of three independent experiments. ** $p < 0.01$; *** $p < 0.001$.

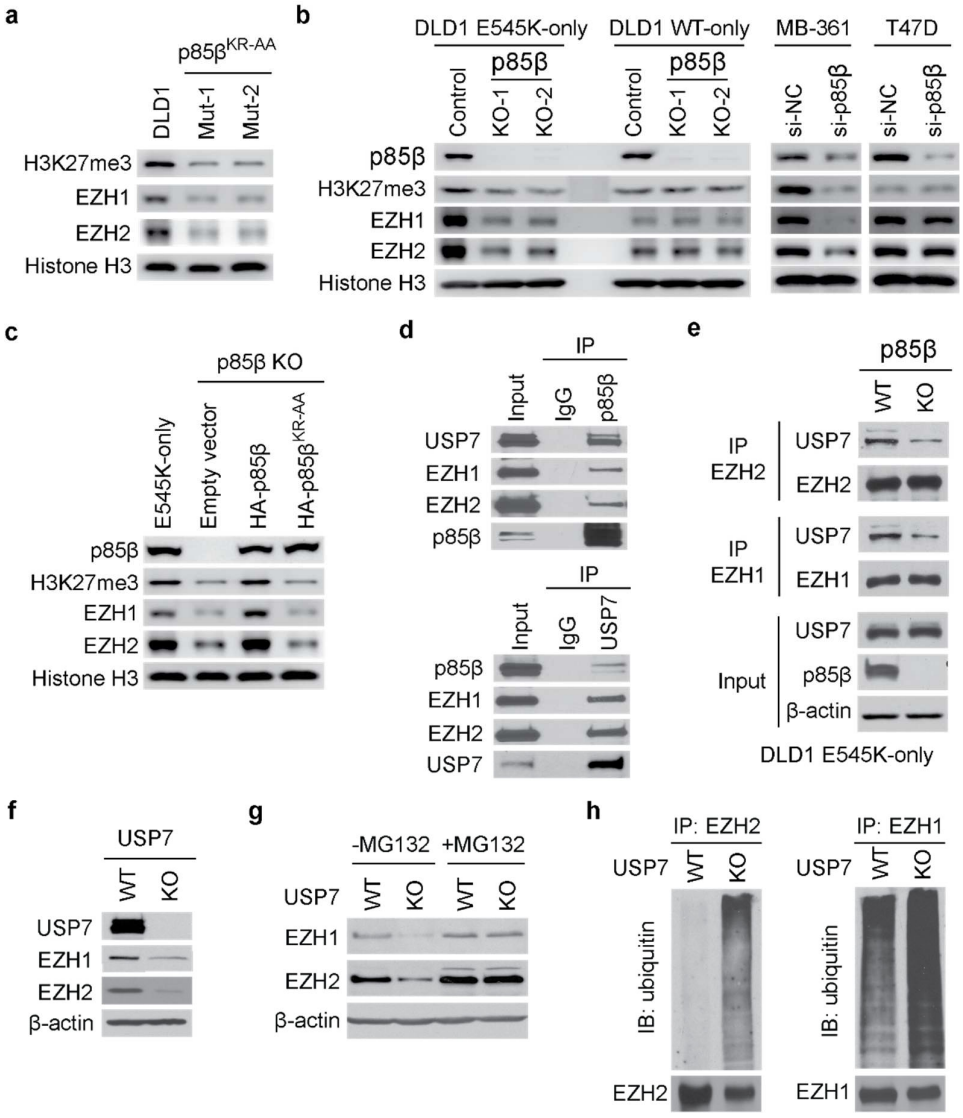

Figure 5. Nuclear p85β recruits the deubiquitinase USP7 to stabilize EZH1/2, increasing H3K27 tri-methylation.

(a-c) Nuclear p85β stabilizes EZH1 and EZH2 and increases histone H3K27 methylation. H3K27me3, EZH1, and EZH2 levels were evaluated by Western blot analyses in indicated cell lines.

(d) Nuclear p85β interacts with USP7, EZH1, and EZH2. DLD1 cells were lysed and immunoprecipitated (IP) with either an anti-p85β or an anti-USP7 antibody, then blotted with indicated antibodies.

(e) The interaction between USP7 and EZH1 or EZH2 is reduced in p85β knockout cells. The indicated cell lines were lysed, IPed with either EZH1 or EZH2, then blotted with indicated antibodies.

(f-h) Deubiquitinase USP7 protects EZH1 and EZH2 from ubiquitin-mediated degradation. Lysates of DLD1 parental cells and USP7 knockout cells were blotted with indicated antibodies (f). DLD1 parental cells and USP7 knockout cells were treated with either vehicle or MG132 for 6 hours and then blotted with indicated antibodies (g). After treated with MG132 for 6 hours, DLD1 parental cells and USP7 knockout cells were lysed, IPed with an antibody against either EZH1 or EZH2, then blotted with indicated antibodies (h).

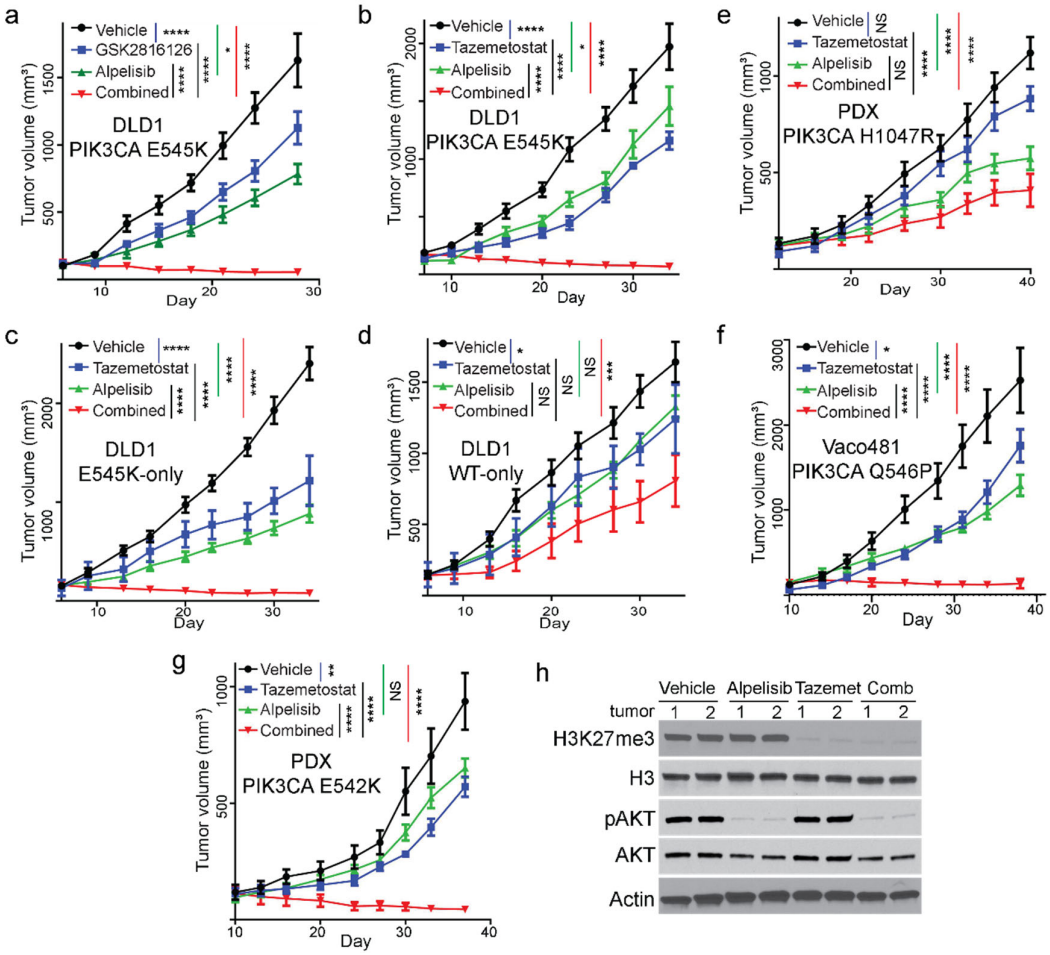

Figure 6. A combination of p110α and EZH inhibitors induces regression of tumors with PIK3CA helical domain mutations, but not WT or kinase domain mutation. **(a)** Subcutaneous xenograft tumors established from DLD1 cells were treated with vehicle or the indicated drugs. GSK2814126: an EZH2 inhibitor; Alpelisib: a p110α-specific inhibitor. (**b** to **g**) Tumors are treated with an EZH inhibitor Tazematostat (EPZ-6438), Alpelisib, or the drug combination. Subcutaneous xenograft tumors established from DLD1 parental cells (b), DLD1 PIK3CA E545K-only cells (c), DLD1 PIK3CA WT-only cells (d); a CRC patient-derived xenograft (PDX) with a PIK3CA H1047R kinase domain mutation (e), Vaco481 CRC cells with a PIK3CA Q546P mutation, or a CRC PDX with a PIK3CA E542K mutation (g). Lysates of PIK3CA E542K mutant PDX tumors treated with the indicated drug were blotted with the indicated antibodies. Statistical analyses, two-way ANOVA. * $p<0.05$; *** $P<0.001$; **** $P<0.0001$; NS, not significant.

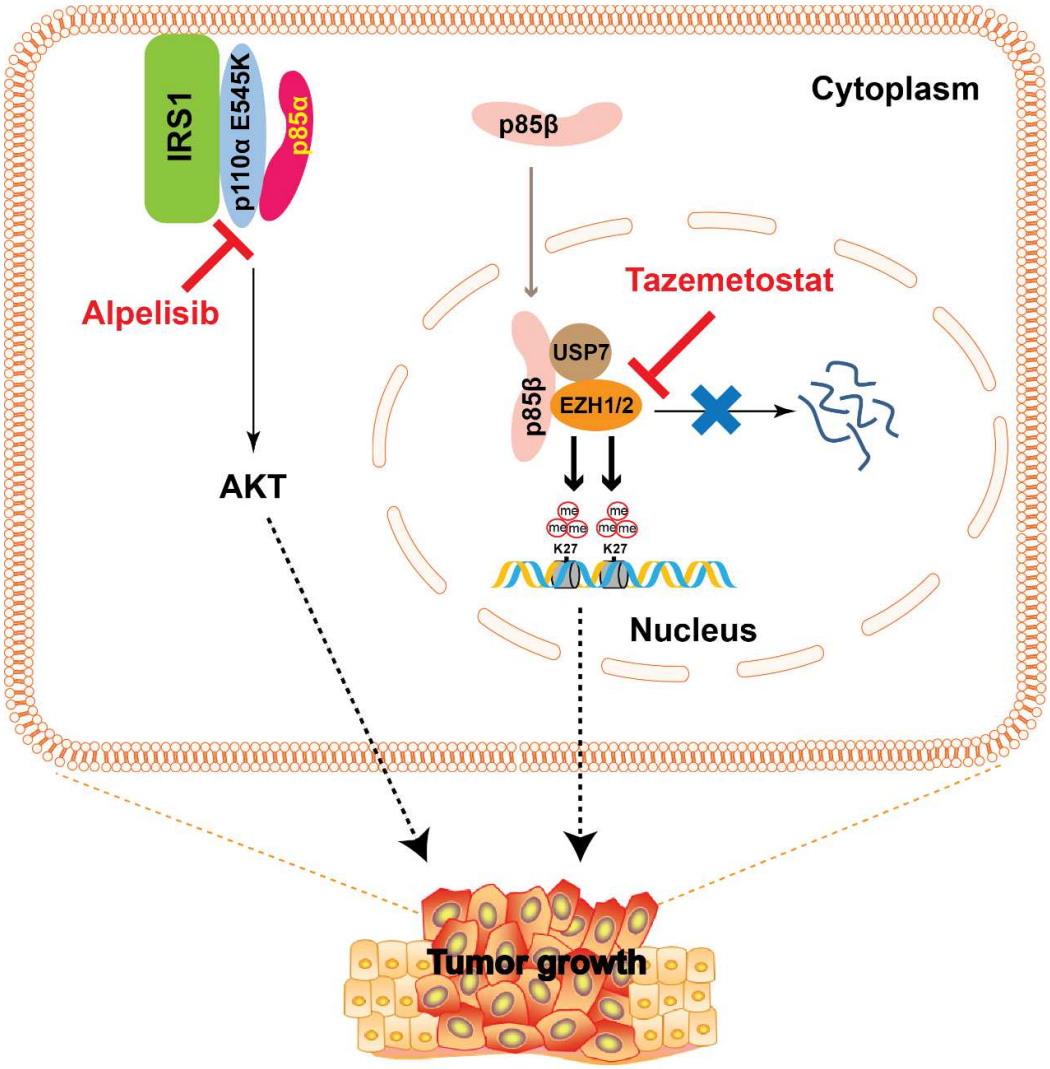

Figure 7. A model for how PIK3CA helical domain mutations promote oncogenesis. PIK3CA helical domain mutations promote oncogenesis through two independent pathways: (1) p110α helical domain mutant protein directly interacts with IRS1 to activate the canonical PDK1-AKT pathway (citation); and (2) p85β translocates into the nucleus, stabilizes EZH1/2 by recruiting deubiquitinase USP7, and enhances H3K27 trimethylation. Simultaneously targeting both pathways with Alpelisib, a p110α inhibitor, and Tazemetostat, an EZH2 inhibitor, induces regression of tumors harboring a PIK3CA helical domain mutation.

Figures

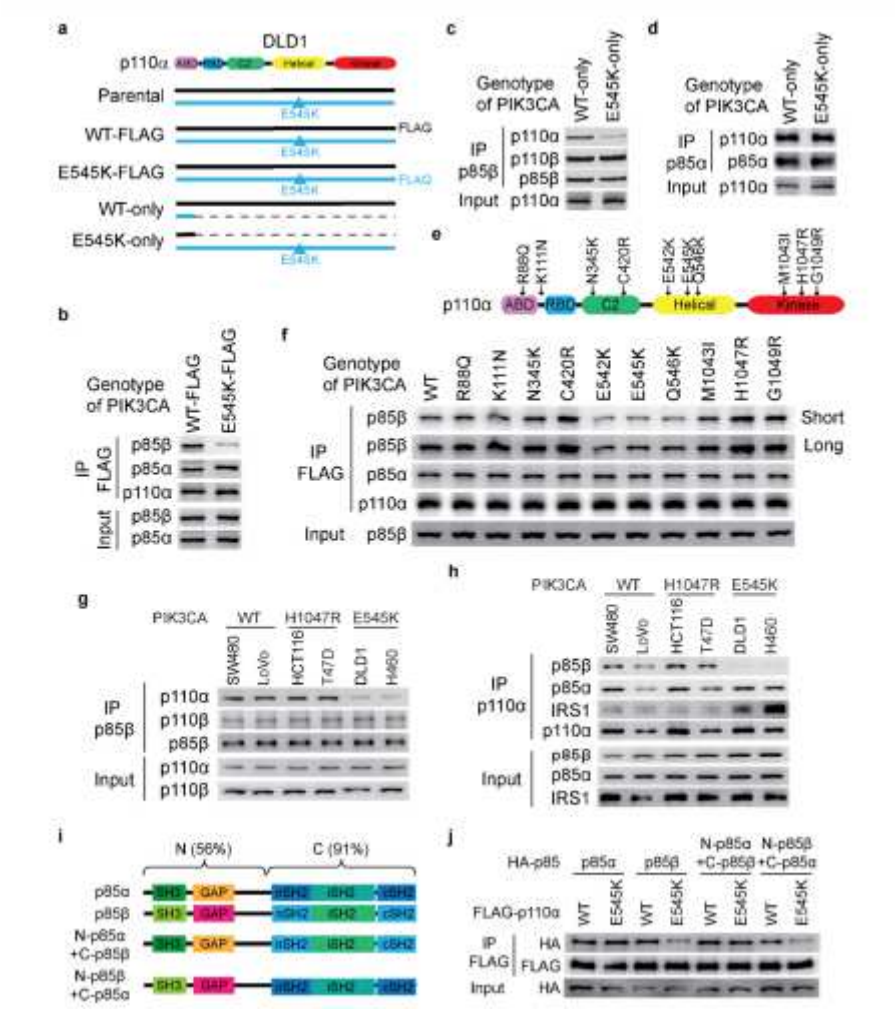

Figure 1

[Please see the manuscript file to view the figure caption.]

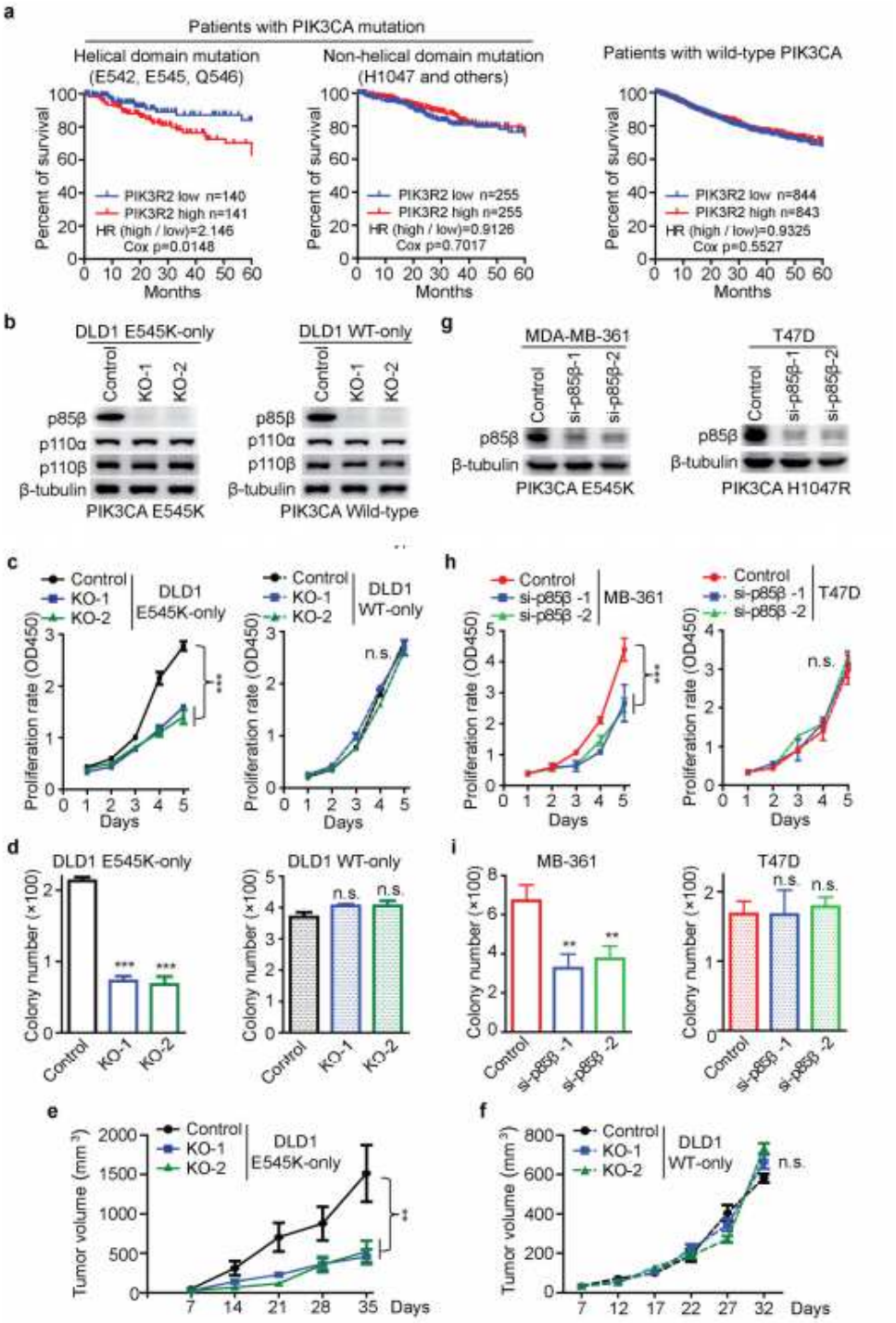

Figure 2

[Please see the manuscript file to view the figure caption.]

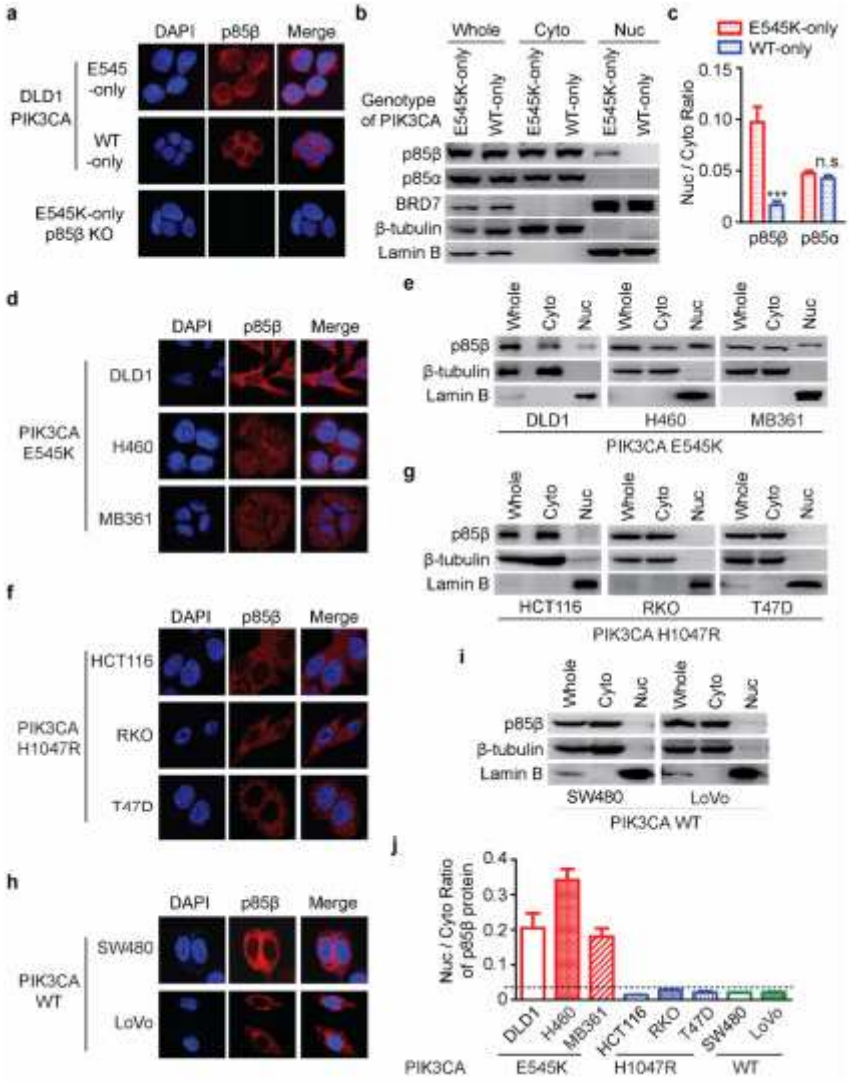

Figure 3

[Please see the manuscript file to view the figure caption.]

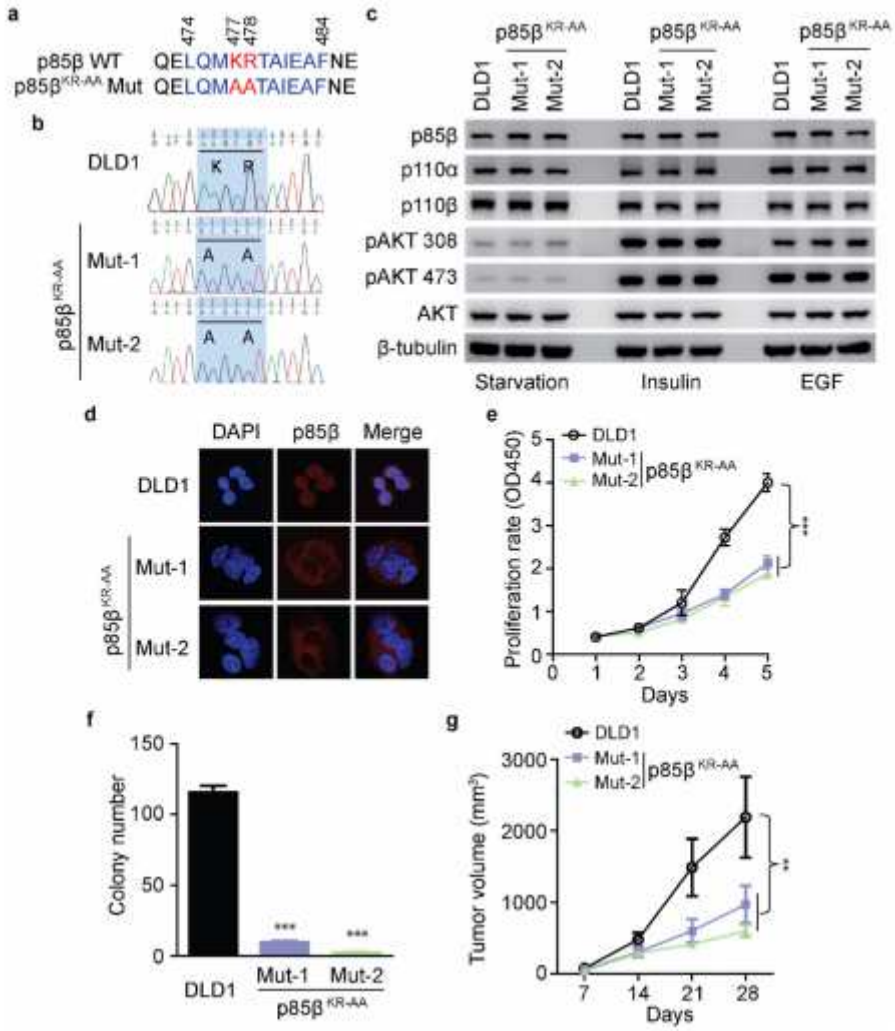

Figure 4

[Please see the manuscript file to view the figure caption.]

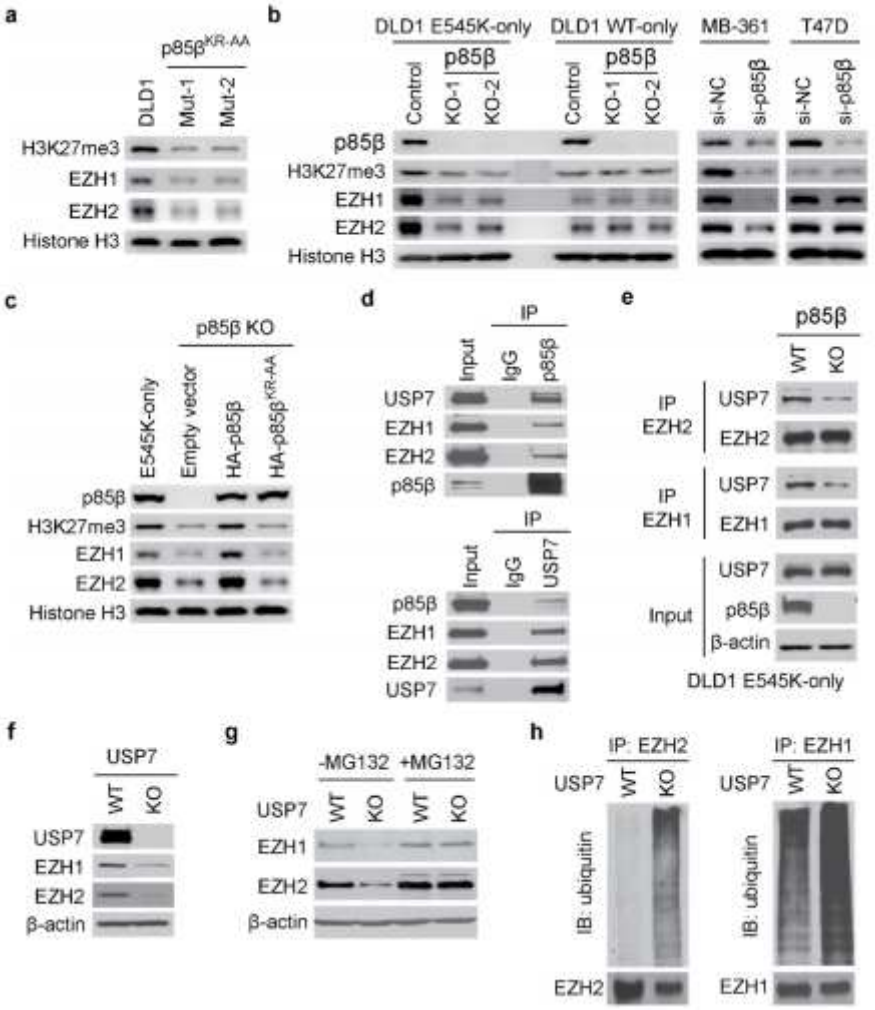

Figure 5

[Please see the manuscript file to view the figure caption.]

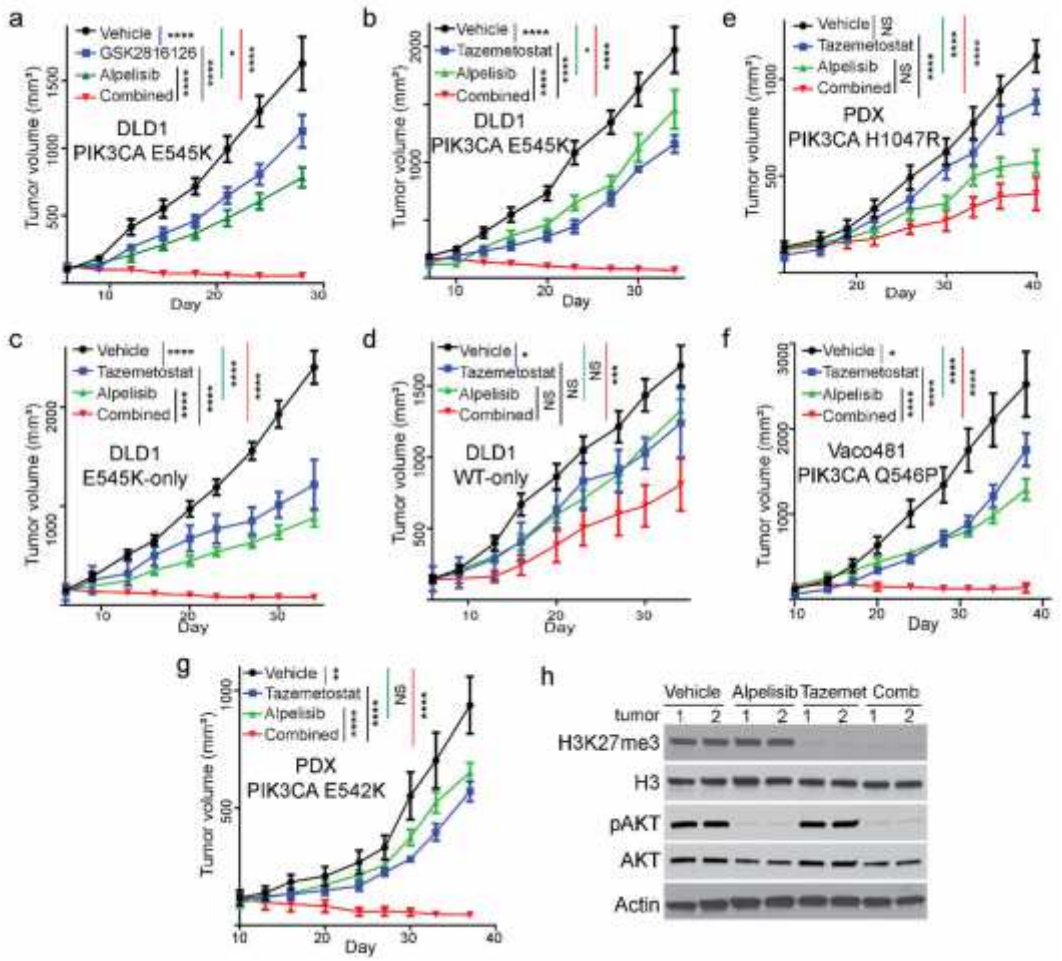

Figure 6

A combination of p110α and EZH inhibitors induces regression of tumors with PIK3CA helical domain mutations, but not WT or kinase domain mutation. (a) Subcutaneous xenograft tumors established from DLD1 cells were treated with vehicle or the indicated drugs. GSK2814126: an EZH2 inhibitor; Alpelisib: a p110αspecific inhibitor. (b to g) Tumors are treated with an EZH inhibitor Tazematostat (EPZ6438), Alpelisib, or the drug combination. Subcutaneous xenograft tumors established from DLD1 parental cells (b), DLD1 PIK3CA E545K-only cells (c), DLD1 PIK3CA WT-only cells (d); a CRC patient-derived xenograft (PDX) with a PIK3CA H1047R kinase domain mutation (e), Vaco481 CRC cells with a PIK3CA Q546P mutation, or a CRC PDX with a PIK3CA E542K mutation (g). Lysates of PIK3CA E542K mutant PDX tumors treated with the indicated drug were blotted with the indicated antibodies. Statistical analyses, two-way ANOVA. * p<0.05; *** P<0.001; **** P<0.0001; NS, not significant.

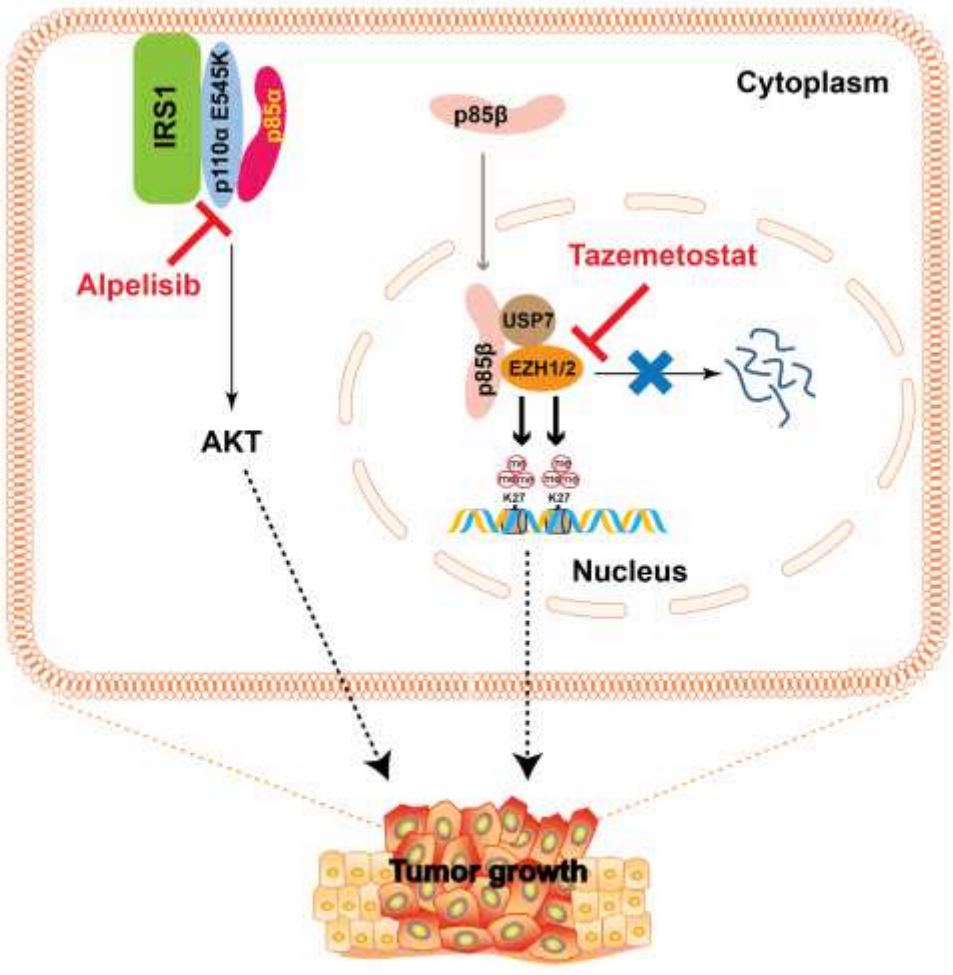

Figure 7

A model for how PIK3CA helical domain mutations promote oncogenesis. PIK3CA helical domain mutations promote oncogenesis through two independent pathways: (1) p110α helical domain mutant protein directly interacts with IRS1 to activate the canonical PDK1-AKT pathway (citation); and (2) p85β translocates into the nucleus, stabilizes EZH1/2 by recruiting deubiquitinase USP7, and enhances H3K27 trimethylation. Simultaneously targeting both pathways with Alpelisib, a p110α inhibitor, and Tazemetostat, an EZH2 inhibitor, induces regression of tumors harboring a PIK3CA helical domain mutation.

Supplementary Files

This is a list of supplementary files associated with this preprint. Click to download.

- SupplementaryMaterials.pdf